# CHAPTER IV

RESULTS AND DISCUSSIONS

4.1   Characterization of synthetic fly ash

4.1.1   Appearance of the melted glass

After the melting process at 1450 °C for 2 hours, the appearance of eight glass compositions was observed. It was found that Class C samples melted homogenous. They were clear glass with blackish brown color with sharp cracks. On the other hand, the Class F samples were harder to melt. Good mixing of the raw materials and pressing them in platinum crucible were required before melting. They had the appearance of black-colored and clear glass with high viscosity.

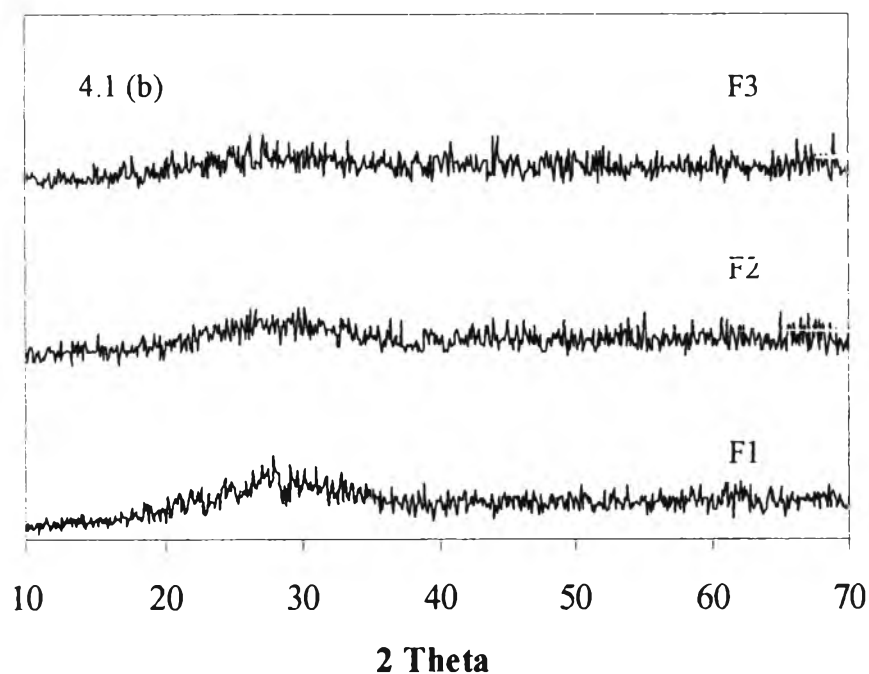### 4.1.2   X-ray diffractometer (XRD)
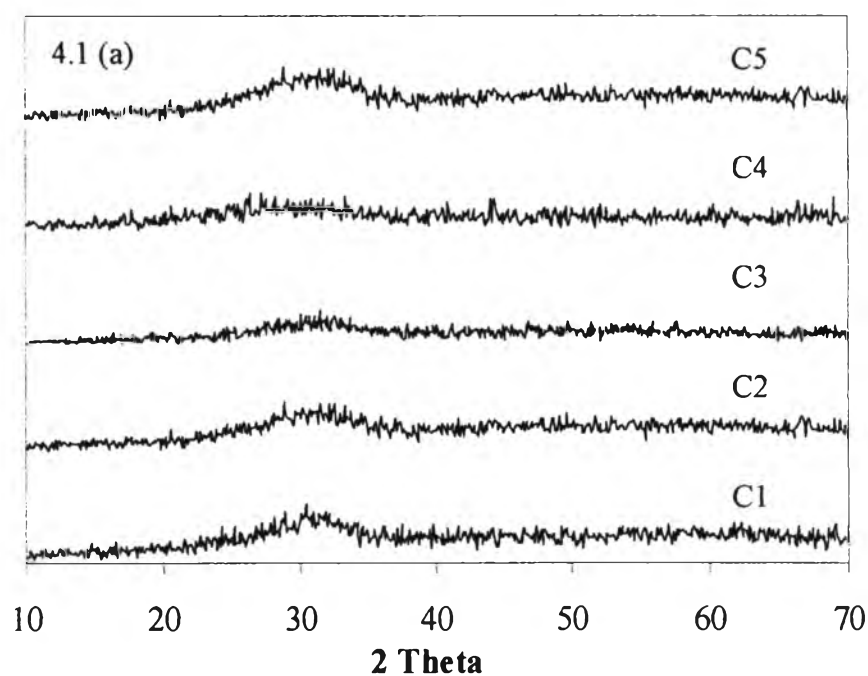
Figure 4.1: X-ray diffractogram of synthetic fly ash (a) Class C and (b) Class F

The mineralogy of the synthetic fly ash was observed by an X-ray diffractometer (XRD). The results are shown in Figure 4.1. It can be seen that these synthetic fly ashes are totally amorphous materials because no crystalline phase is presented in the diffractogram.

4.1.3 X-ray fluorescence spectrometer (XRF)

The bulk chemical composition of synthetic fly ash determined by an X-ray fluorescence (XRF) spectroscopy is shown in Table 4.1. The values are expressed by the weight percentage in oxide forms and normalized to 100%. The chemical compositions in synthetic fly ash are SiO_2, AlO_3, Fe_2O_3, CaO, Na_2O, K_2O, MgO, and SO_3. The actual composition is compared with the mixed composition in the Figure 4.2. It was found that the ratio of $SiO_2/Al_2O_3/Fe_2O_3$ and CaO/Na_2O+K_2O of the actual composition does not vary much from the target compositions.

Table 4.1: Total chemical composition of synthetic fly ash determined by an XRF. Values are expressed as weight percentage normalized to 100%

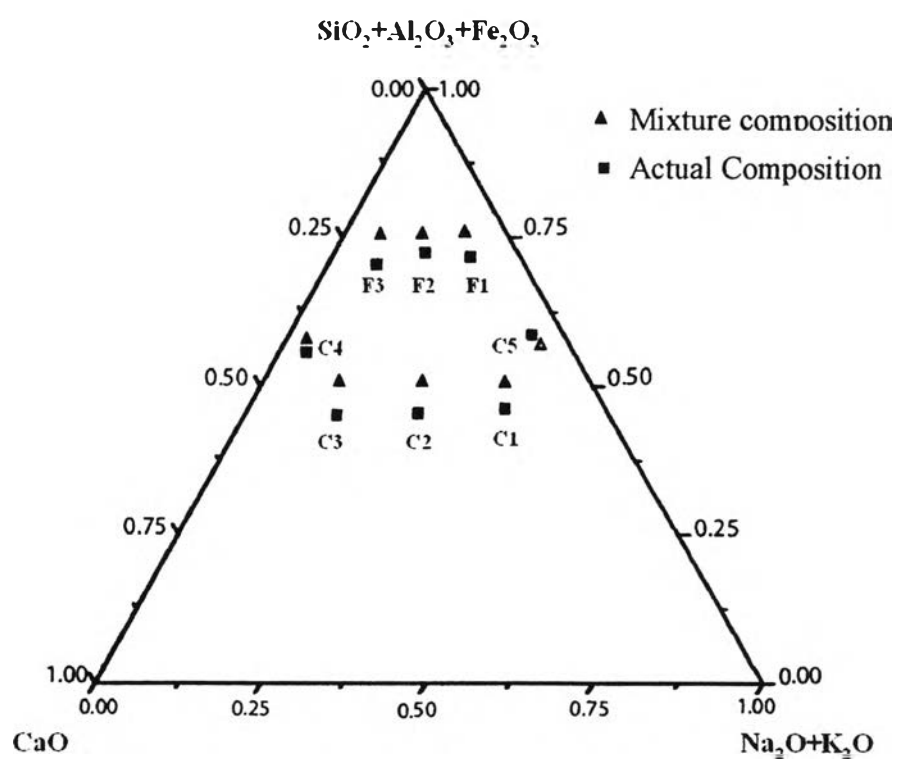| Sample	SiO₂	Al₂O₃	Fe₂O₃	MgO	SO₃	CaO	Na₂O	K₂O
C1	26.30	12.90	6.13	1.31	0.56	14.90	18.02	19.80
C2	25.70	12.90	5.71	1.40	0.51	27.80	11.90	13.40
C3	25.70	13.10	5.34	1.56	0.40	40.10	7.10	6.54
C4	30.77	16.53	7.12	1.81	0.29	39.40	1.99	1.88
C5	32.20	17.43	7.56	1.90	0.39	4.81	17.13	18.40
F1	39.70	22.30	8.19	1.61	0.44	7.42	10.70	9.55
F2	40.70	22.60	7.36	1.88	0.43	13.60	6.72	6.50
F3	38.10	21.10	9.47	1.75	0.66	21.70	4.24	2.85

Figure 4.2: Ternary Diagram of synthetic fly ash composition.

4.1.4 Particle size analysis

The particle size of synthetic fly ash powder, which was passed through sieve number 200-325 mesh (45-75 micron openings), was measured by a particle size analyzer. The particle size distributions of Class C and Class F synthetic ashes are shown in Figures 4.3 (a) and 4.3 (b), respectively.
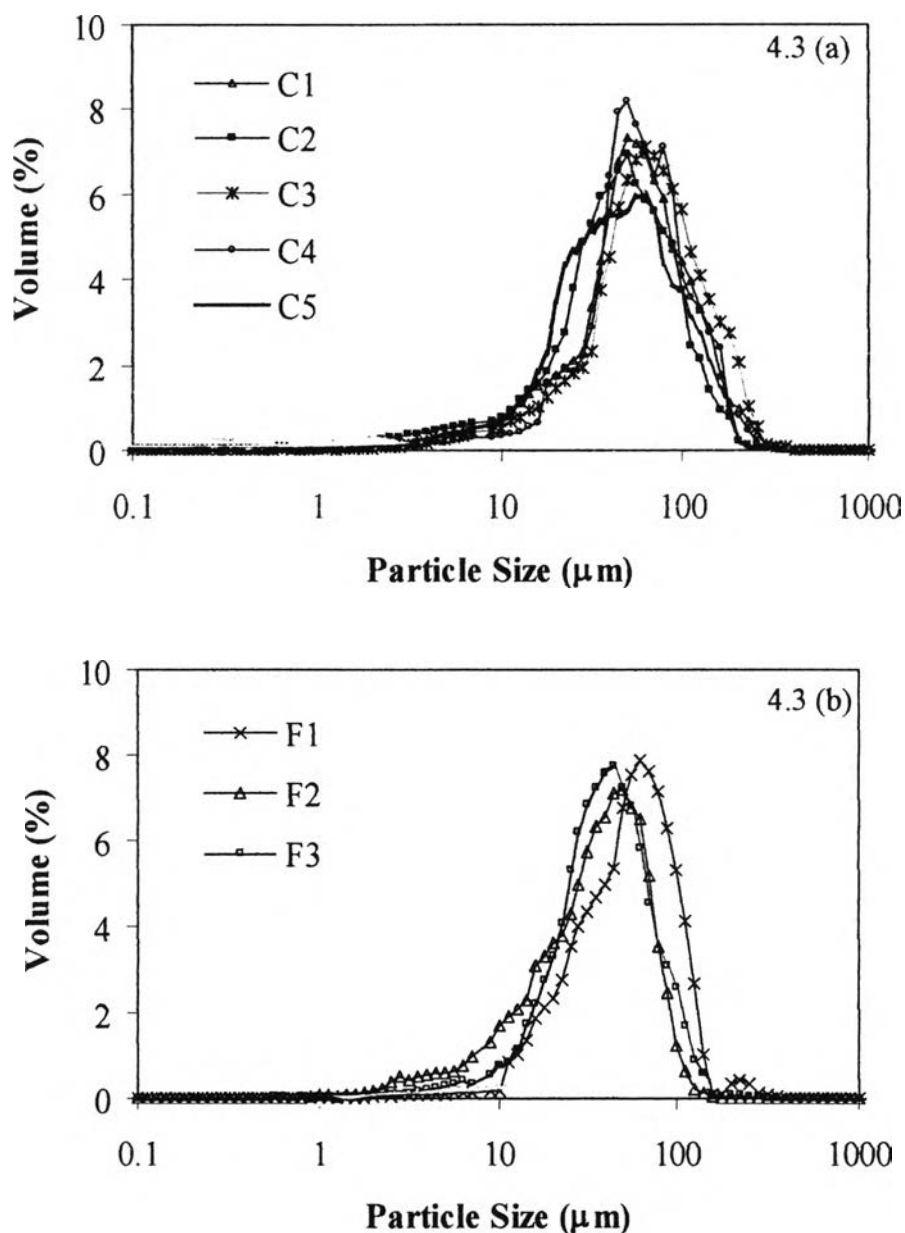

Figure 4.3: Particle size distribution of synthetic fly ash (a) Class C and (b) Class F.

From Figures 4.3, it was found that particle size of synthetic fly ash Class C varied from 5 to 300 μm. The majority of particle fell in the range of 50-80 μm. The mean particle size of C1, C2, C3, C4, and C5 were about 50, 50, 60, 50, and 63 μm, respectively. The particle size of those Class F was varied from 3 to 150 μm. The mean size of F1, F2, and F3 were 60, 50, and 45 μm respectively. The particle size distributions of Class C seem to be broader than Class F and that of C5 was very broad comparing with the others in the same series.

4.1.5 Porosimeter

The surface area of synthetic ash is one of the properties that control the leaching. The porosity of synthetic fly ash powder, which passed through sieve number 200-325 mesh (45-75 micron openings), was measured by the Porosimeter. The data are reported in in m^2/g as shown in Table 4.2. It can be seen that the surface area of synthetic fly ash falls in the range of 0.632-0.776 m^2/g with the correlation coefficient at 0.97019-0.99992.

Table 4.2: Surface area of synthetic fly ash determined by the porosimeter

Sample	Surface Area (m^2/g)	Average surface area	S.D.
C1	0.688		
C2	0.734		
C3	0.658	0.684	0.03
C4	0.673		
C5	0.668		
F1	0.632		
F2	0.776	0.69	0.076
F3	0.663		

From Table 4.2, it was shown that C2 has the highest surface area of 0.734 m^2/g for Class C and F2 has the highest surface area of 0.776 m^2/g for Class F. Both series had lower standard deviation within the series assuring that the surface area would not be a major factor varying the leaching among glasses. The average surface area and standard deviation for Class C was 0.684 m^2/g and 0.03, respectively. In the Class F series, the average surface area was 0.69 m^2/g and the standard deviation was 0.076.

4.1.6 Density

The factors which affect the density are the structure, bonding, and composition of a material including the cooling rate of the glass as well. Large atoms, short bond lengths, and compact structures lead to high density values. While a glass with a faster cooling rate tends to be of lower density (Mauro, 2000). Since density relates to the composition, it can be used to define the reactivity of glass which depends on composition. The densities of glass samples are shown in the following table.

Table 4.3: Density of synthetic fly ash

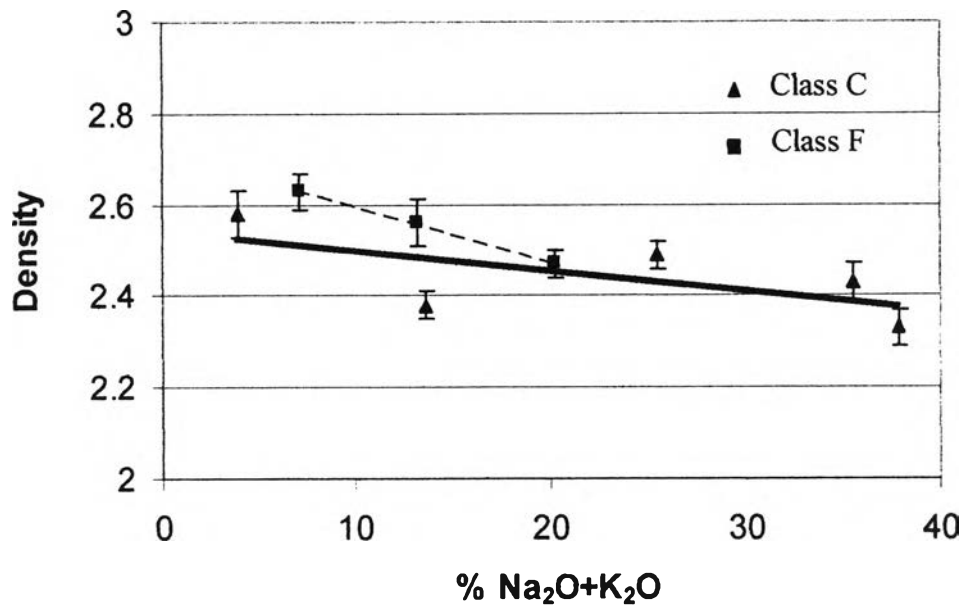| Sample	C1	C2	C3	C4	C5	F1	F2	F3
Density (g/cm³)	2.33	2.49	2.38	2.43	2.58	2.47	2.56	2.63
S.D.	0.02	0.01	0.01	0.04	0.02	0.01	0.03	0.02

Figure 4.4: Density of synthetic fly ash at different amount of alkalis

The true particle density (TPD) of real fly ash can range from 0.8 to 4.0 g.cm^{-3} (Hemmings and Berry, 1986) and from 2.02 to 2.59 g.cm^{-3} for fly ash in Thailand (Committee of Civil Engineering Department, 2000). From Table 4.3, it can be seen that the density of synthetic fly ashes falls within this general range. These synthetic fly ashes have a density in range of 2.33-2.63 g.cm^{-3} and their standard deviation was in range of 0.001-0.004. In Figure 4.4, it was found that the density of Class F was higher than that of Class C. When considering within Class F or Class C itself, it can be concluded that the density of synthetic fly ash decreases with an increasing alkalis content. The presence of alkalis tends to create a highly open glass network, which increases the volume of glass and decreases its density (Mauro, 2000).

4.1.7 Refractometer

A refractometer was used to determine the refractive index, which is the ratio between the speeds of light in a vacuum per the speed of light in a material. A high refractive index indicates a large reduction in the speed of light. The refractive index of glass samples are shown in the following table.

Table 4.4: Refractive index of synthetic fly ash

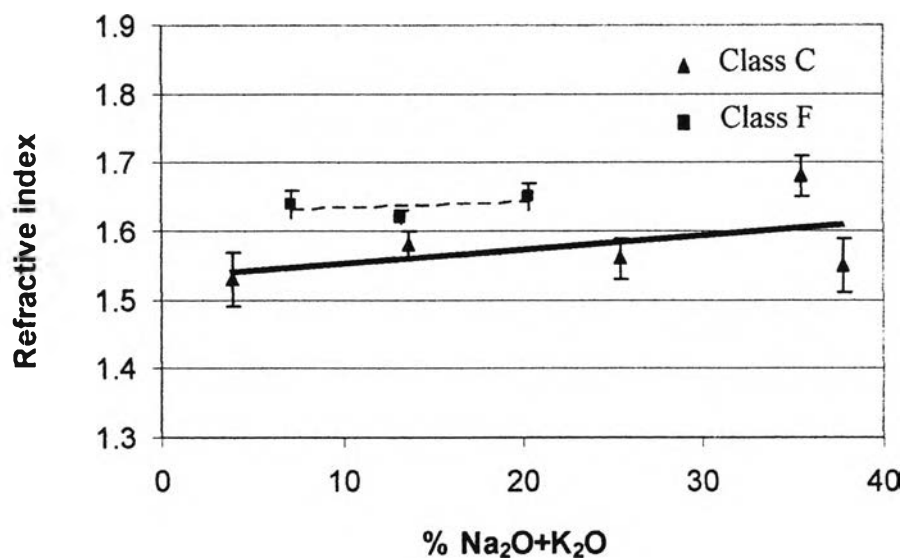| Sample	Refractive index
C1	1.55 ± 0.02
C2	1.56 ± 0.01
C3	1.58 ± 0.02
C4	1.53 ± 0.04
C5	1.68 ± 0.03
F1	1.65 ± 0.04
F2	1.62 ± 0.03
F3	1.64 ± 0.02

Figure 4.5: Refractive index of synthetic fly ash at different amounts of alkalis

From Figure 4.5, it can be seen that the refractive index values tend to increase as the alkalis ions increase. This is because polarizable species can retard the light through the material. Weak bonding and low network connectivity leads to a larger refractive index value as well (Mauro, 2000). The refractive index of glass is influenced not only by its chemical components but also by the cooling process used when it was produced (Suzuki et al., 2000).

4.2 Leaching rate of synthetic fly ash

In the SPFT leaching experiment, eight synthetic fly ash compositions and three interval pH values were used. The samples were tested for 28 days with two duplicates. The concentrations of element in the leachate measured by an ICP are presented in ppm. These raw data are shown in Appendix A. These leaching rates were calculated using the following formula (McGrail et al., 2000):

$$\text{The leaching rate } (g.m^{-2}.d^{-1}) = (C_i - \overline{C_{i,b}})q / (f_i S) \quad\quad (4.1)$$

where C_i is the concentration of the element i in the effluent (g/L^{-1}); $\overline{C_{i,b}}$ is the average background concentration of the element of interest (g/L); q is the flow-through rate (L/d); f_i is the mass fraction of the element in glass (dimensionless); and S is the surface area of the sample (m^2). The example for leaching rate calculation is shown in Apppendix B.

Since the SPFT is the leaching test with a continuous flow, the leaching process never cease completely (Barkatt, et al, 1988). However, most corrosion reactions occur under the condition of a very slow flow rate, which may eventually reach a steady state and becomes saturation condition. Due to the high possibility of precipitation that could be disturbed the system, the MINEQL+ (V. 4.5) program was chosen to investigate the reaction.

This program also provides the type of components that could occur during the leaching test. The concentration of elements in the leachate was observed daily. Some output from the MINEQL+ program is shown in the Appendix C. This report compiles the output data of C4 leachate at a pH of 11.5. It can be seen that they were consisted of various species i.e. components, complexes, precipitated solids, and dissolved solid. Most of them were soluble species except the Hermatite and Chrysotil which present as precipitated solid. They are insoluble compounds of Fe and Mg, respectively.

The plot of formations of each element at different pH is also presented. The total line in each picture shows the total solubility of that species at different pH. It shows that Na and K were soluble at all pH. Between pH 11.5 to 12, the Si could formed much of the H_3SiO_4 and some $Si(OH_4)$ and $H_2SiO_4^{2-}$. When pH increased to 12.5, the formation of H_3SiO_4 was reduced and converted to $H_2SiO_4^{2-}$. At pH 11.5, Al might be in a form of Diaspore since it is an insoluble at this pH. However at higher pH of 12-12.5, the soluble $Al(OH)^{4-}$ could be formed. For Fe and Mg species, they can only being a solid form at this pH range. Thus the total line was almost zero. For Ca, it could be present in a form of Ca^{2+} and $CaOH^+$ at this pH range. Thus, the Mineq+ output shows that the elements of concern, Si, Al, Na, K and Ca, were presented in the soluble form and did not form a precipitate. Thus the measured concentration of each element data can be used to compare the leaching among glasses.

The dissolution rate of the released elements as a function of time for the synthetic fly ash Class C is presented in the following Figures.
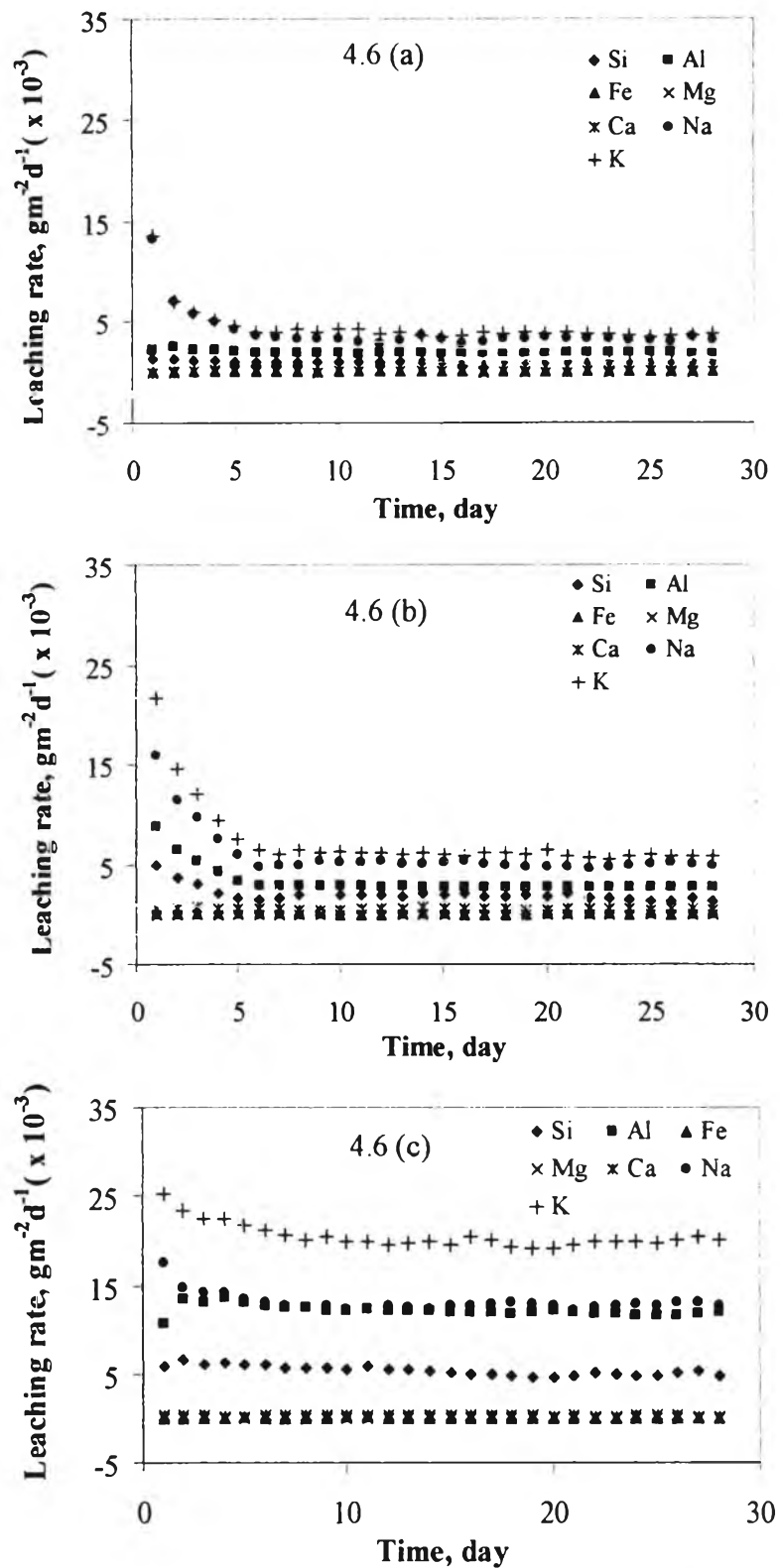
Figure 4.6: Leaching rates of each element as a function of time from the synthetic fly ash Cl at (a) pH = 11.5, (b) pH = 12, and (c) pH = 12.5

Figure 4.6 shows the leaching rate of elements as a function of time of C1 at pH 11.5, 12, and 12.5. The order of them on leaching rate were K>Na>Al>Si>Ca>Mg>Fe. Their leaching rates started with high value and rapidly decreased during the first five days. Then they attained a steady state. This profile is present in leaching rate at pH 11.5 and 12 but not obvious in leaching rate at pH 12.5. Leaching rate of all elements decreased and then became stable. It is also found that the leaching rate of each element was strong dependent on pH. The leaching rates during the steady state condition of all components increased two folds when the pH changes from 11.5 to 12 and was raised another two folds when the pH increased from 12 to 12.5.

In interdiffusion mechanism, the alkali ions, K and Na, in the glass were replaced by hydrogen ions from the solution. The remaining silicate formed hydrated silica rich layer in the subsurface of the glass. The thickness of hydrated silica layer depends on the amount of released alkalis. The initial rate can represent both the diffusion of Na and K and the dissolution. The diffusion rate was high since C1 is rich in Na and K. This high interdiffusion rate left thick layer of silicate hydrate gel where the released Ca and Mg could precipitate in this gel obstructing other species to diffuse out further. As a result, the leaching rate dropped significantly.

At low pH of 11.5 and 12, the rate of silica dissolution or gel removal was not high; therefore, the precipitate of Ca and Mg phase in this gel could block the diffusion resulting high reduction of the leaching rate. Whereas, at high pH of 12.5, the dissolution rate of silica in hydrated silicate gel could be much higher than the rate of Ca and Mg precipitate, resulting thinner silicate gel. Thus, both the diffusion and the dissolution could proceed at the high rate simultaneously and continuously with only small reduction in leaching rate at the beginning.

It has been found by Hench, 1988 that the presence of Ca and Al greatly reduced the thickness of the silica-rich layer, and also reduced the dissolution rate of silica (Hench, 1988). It has been experimentally recognized that the surface composition has a major impact on the durability of glass. The presence of Ca and Al can form the secondary film or dual film cover on the surface of the glass. It can inhibit the Na and K ion exchange reaction and restrain the breaking of silica bonding as well. Fe and Mg barely appeared in the solution. Their concentrations were below the detection limit because they were likely to remain or re-precipitate on the glass surface, but in certain case they formed as colloids away from the surface. At pH 11.5-12.5, Fe and Mg were present in the formation of Hermatite and Chrysotil as shown by the MINEQL+ program in Appendix C.
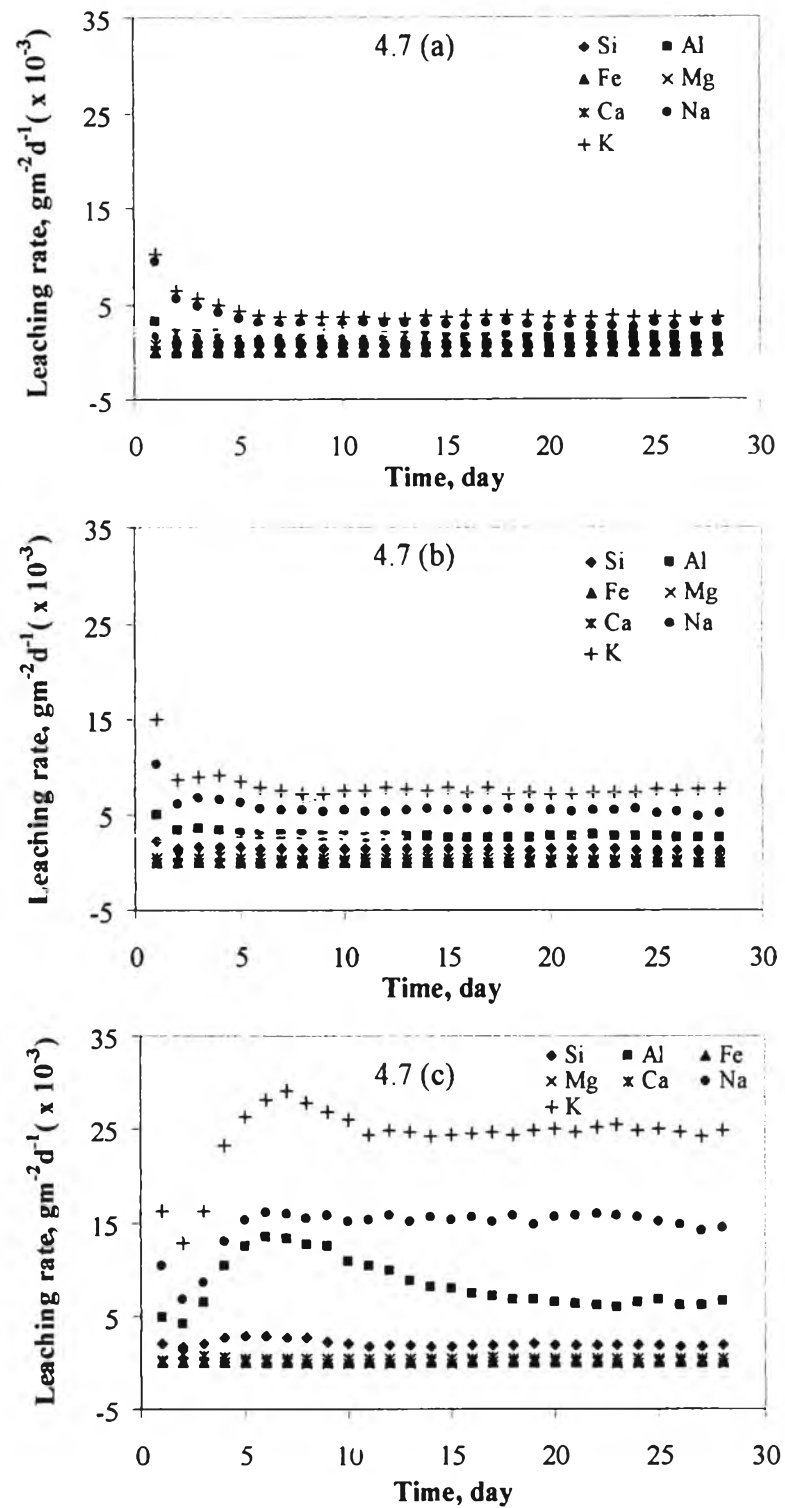
Figure 4.7: Leaching rate of each element as a function of time from the synthetic fly ash C2 at (a) pH = 11.5, (b) pH = 12, and (c) pH = 12.5

Figure 4.7 shows the leaching rate of elements as a function of time of C2 at pH 11.5, 12, and 12.5. The order of the leaching rates were K>Na>Al>Si>Ca>Mg>Fe. At pH 11.5, the leaching rates started at high value and rapidly decreased to steady state. The same concept of leaching rate at low pH in C1 can be applied here. However the profiles of pH 12 and 12.5 are different. These leaching rates started with the low value. It was possibly due to low diffusion of Na and K in this low alkalis glass. The leaching rates increased later as dissolution proceeds. After two days for pH 12 and five days for pH 12.5, the leaching rates dropped. The leaching rate of pH 12.5 could proceed at high rate at longer time since the glass was attacked by higher hydroxyl ion concentration. The leaching rates slightly reduced by the precipitate in the gel and became steady state at high rate.

These leaching rates were also strong dependency to pH. The leaching rate of K and Na showed a double increase when the pH changed from 11.5 to 12 and three-time increase when the pH rose to 12.5. Nevertheless, the leaching rates of the others components increased in lower degree than when pH altered from 11.5 to 12.5.
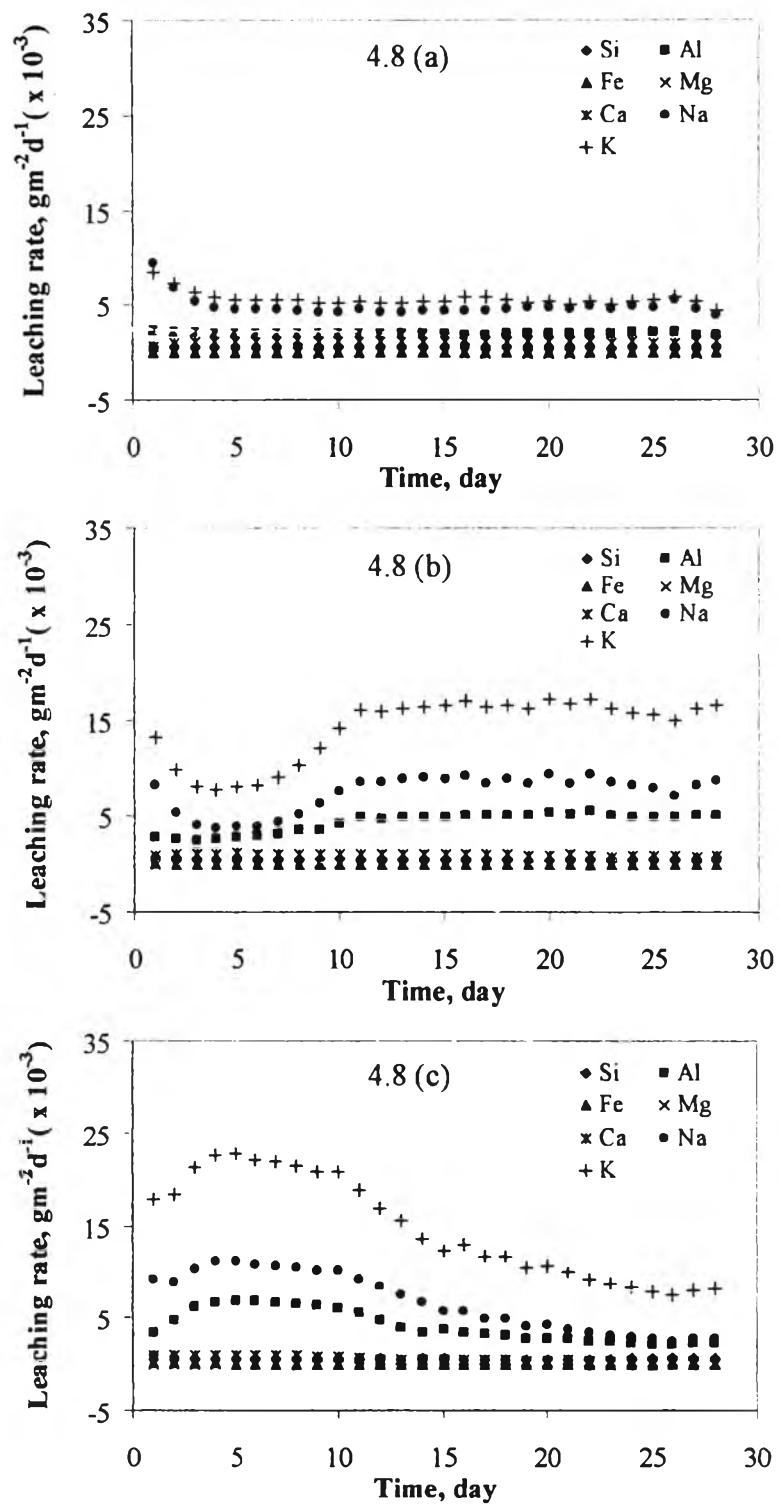
Figure 4.8: Leaching rates of each element as a function of time from the synthetic fly ash C3 at (a) pH = 11.5, (b) pH = 12, and (c) pH = 12.5

Figure 4.8 shows the leaching rate of various elements from sample C3 at pH 11.5, 12, and 12.5. The order of the leaching rates were K>Na>Al>Ca>Si>Mg>Fe. Similar trend was observed in pH 11.5. The leaching rate started with high value and dropped significantly suggesting that the diffusion mechanism was dominant but Ca and Mg phase precipitated in the hydrated silicate gel blocked the diffusion mechanism and slowed down the diffusion. The dissolution of this phase proceeds very slow due to the low pH.

The profile at pH 12 shows two incidents of high leaching rate. The first high leaching rate at the beginning cannot be explained at this point. For the second incident, since this glass had lowest content of Na and K, thus, its diffusion rate would be very low at the beginning. It did not torm a hydrated silicate gel so dissolution could not proceed at high rate resulting in the delay for seven day before dissolution could take place. Then it continuously proceeds with the same rate.

Interesting result was found at pH 12.5. Similar to the C2 result at pH 12.5 that the diffusion and the dissolution precede at high rate simultaneously. However the leaching rate slowly dropped to almost zero for all species. This could be due to the large formation of Ca or Al phase in the subsurface layer in this rich calcium glass. The evidence of these phases could be observed in future research. The leaching rate increased a bit when the pH changed.
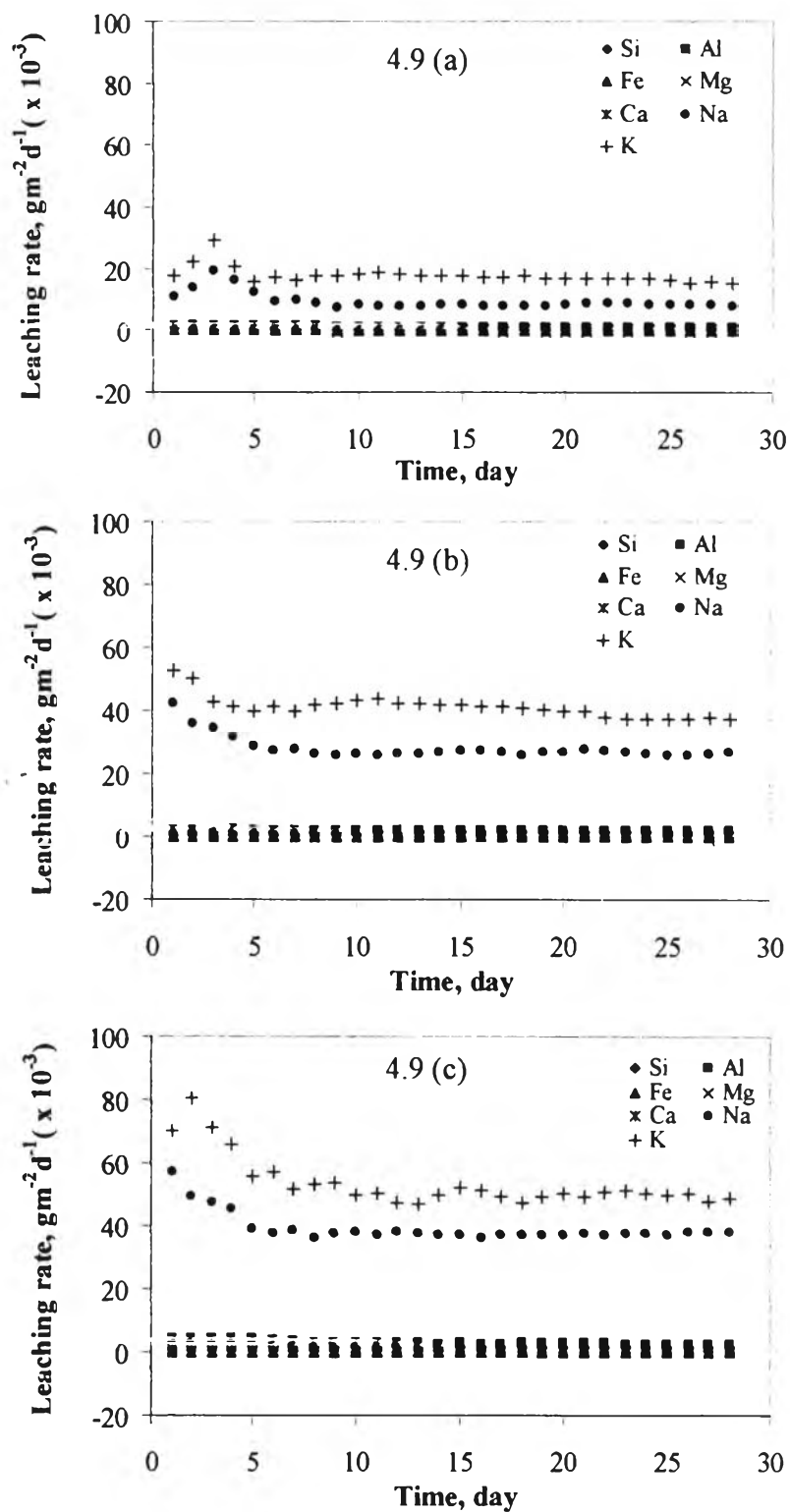
Figure 4.9: Leaching rates of each element as a function of time from the synthetic fly ash C4 at (a) pH = 11.5, (b) pH = 12, and (c) pH = 12.5

The leaching rate of synthetic fly ash C4 at different pH values is shown in the Figure 4.9. The order of the leaching rate was similar to other glasses. The leaching rates of K and Na started at high value at beginning and dropped out sharply at later age as a result of precipitate obstruction. When comparing with other components in the same series, the leaching rates of K and Na was much higher. The pH value had a significant effect on the leaching rate of K and Na but it had a small effect on the other components. In C1, C2, and C3, other elements could diffuse out in somewhat amount. However the elements in C4 could not dissolve out even at high pH. It might be due to its strong bonding of silicate aluminate species forming from high the Al/Si ratio. As shown in Table 4-6, the Al/Si ratio of sample C4 and C5 was higher than the others in the same series. Therefore, dissolution of this strong silicate in hydrated gel hardly occurred. On the other hand, the diffusion might form a hydrated silicate gel inside but it was so strong that hydroxyl ion could not break the bond. As a result, the other elements still remained in the glass and only the diffusion of Na and K proceeded. The strong bonding was expected since this glass contained very low percentage of network breaker or Na and K.
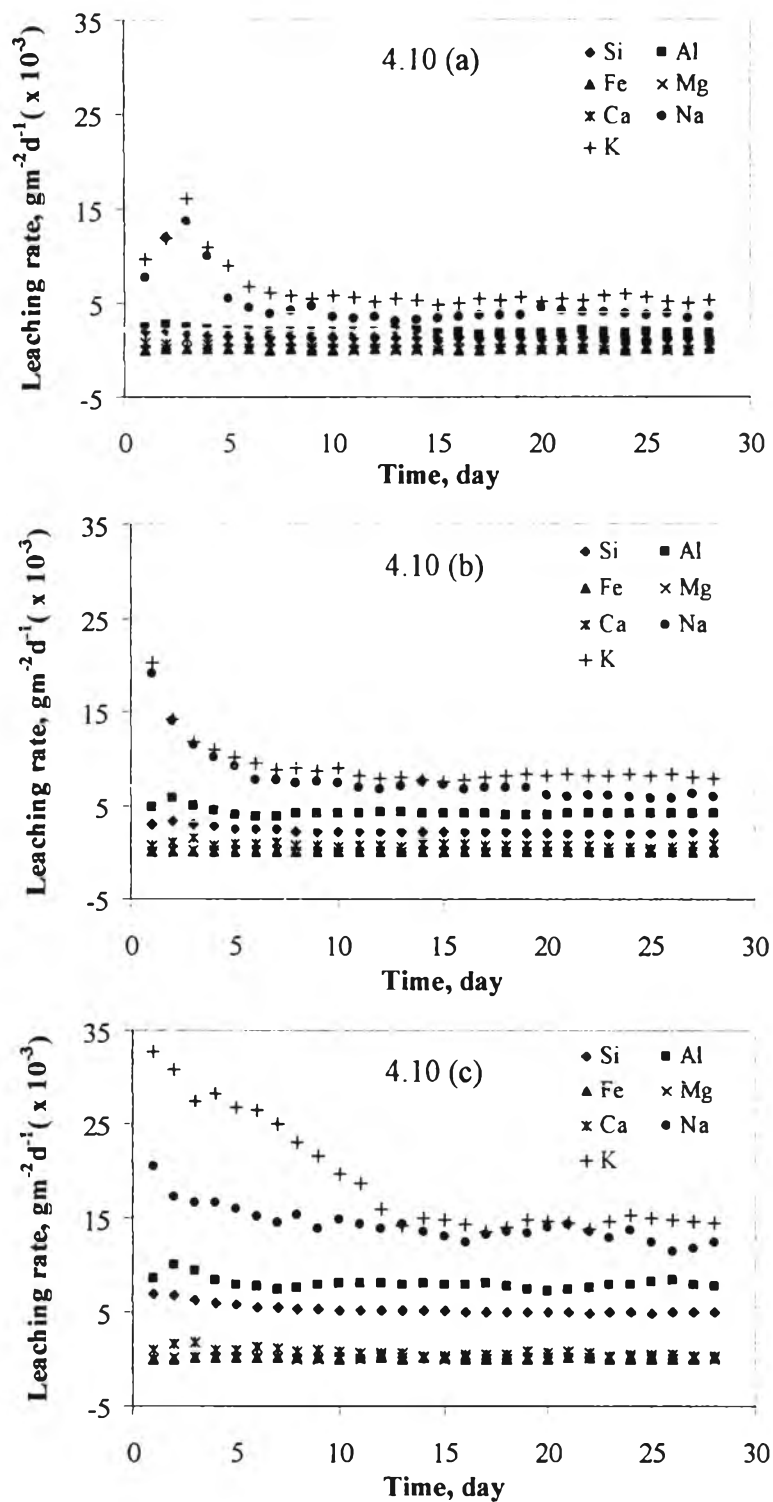
Figure 4.10: Leaching rates of each element as a function of time from the synthetic fly ash C5 at (a) pH = 11.5, (b) pH = 12, and (c) pH = 12.5

The leaching rate of each element of sample C5 at pH 11.5, 12, and 12.5 are exhibited in Figure 4.10. The order of the leaching rate was the same as other samples where K> Na >Al> Si>Ca>Mg>Fe. The leaching rate of Na and K proceeded to the maximum at the first three days and rapidly declined to constant value. The others seem to be stable with time. It had a small effect on the leaching rate when the pH changed from 11.5 to 12. However it was more significant at a pH of 12.5; the leaching rate was double increased. Its leaching profile could be compared to that of C4 to investigate the effect of alkalis content as they both had the same Al/Si but different in the alkalis content. These two glasses had the same leaching profiles but there were higher leaching rate of the other components in C5. This could be due to the high Na and K in C5. Although it had a high Al/Si but it was composed of a very high alkalis content that its silicate structure became weak. Thus its silicate bonding in hydrated silicate gel was prone to attack by hydroxyl ion more. As a result, the dissolution of hydrated silicate gel proceeded at greater rate allowing the other elements to diffuse out of the glass.

The leaching rate at steady state is used in comparison among glasses as the obstruction by phases in subsurface layer already took place. A comparison these steady state leaching rates within Class C series found that the leaching rate order of Si was C4<C3<C2<C1<C5. This followed the order of Na and K content in their glasses. Thus, it agreed with Barkatt's paper that the dissolution rate of glass in aqueous media was highly dependent on the presence of components that raise silica solubility (i.e. Na, K) or inhibit it (i.e. Ca, Al) (Barkatt et al., 1988).

The dissolution rate of the released elements as a function of time for the synthetic fly ash Class F is presented in the following Figures.
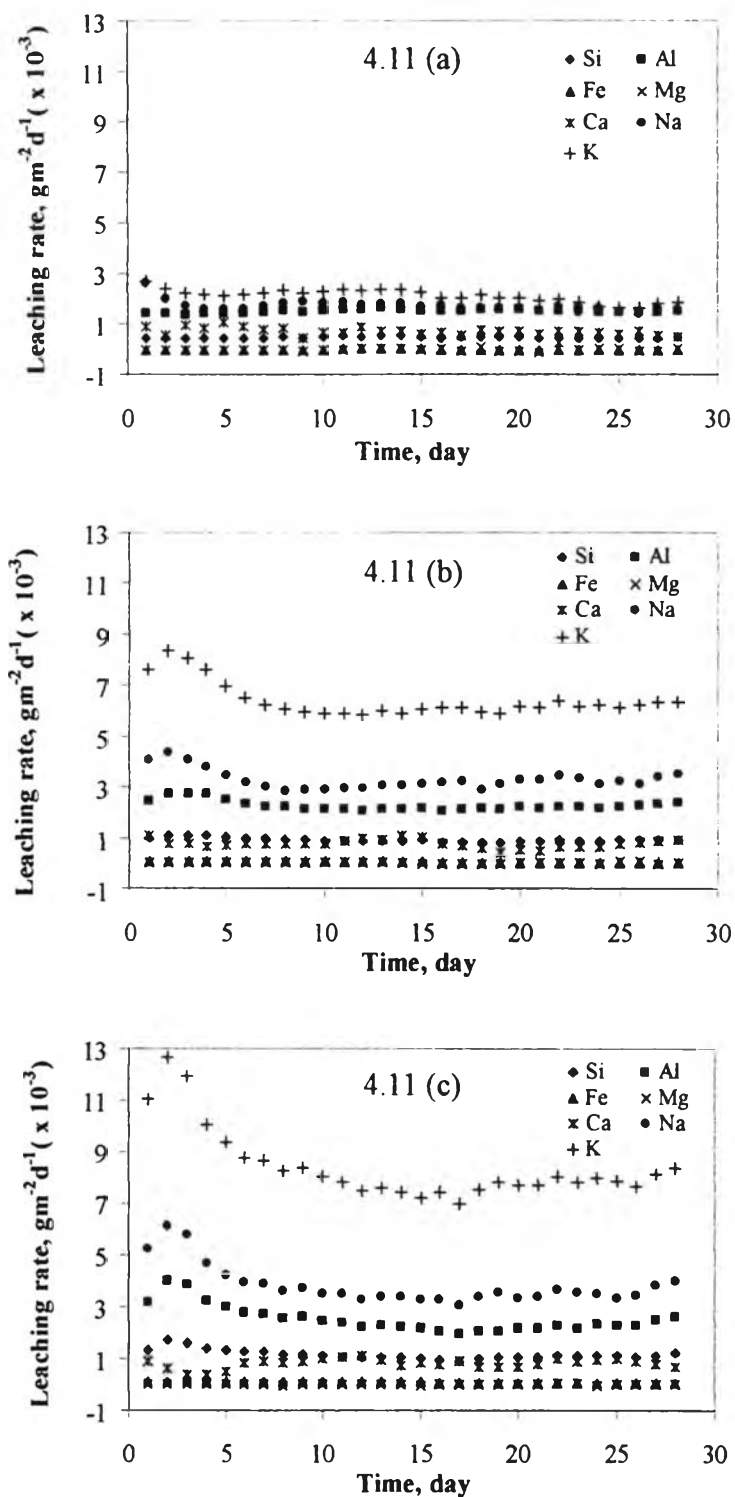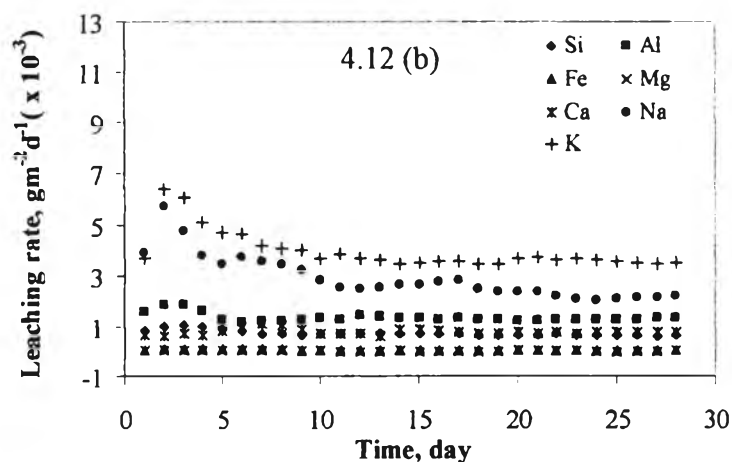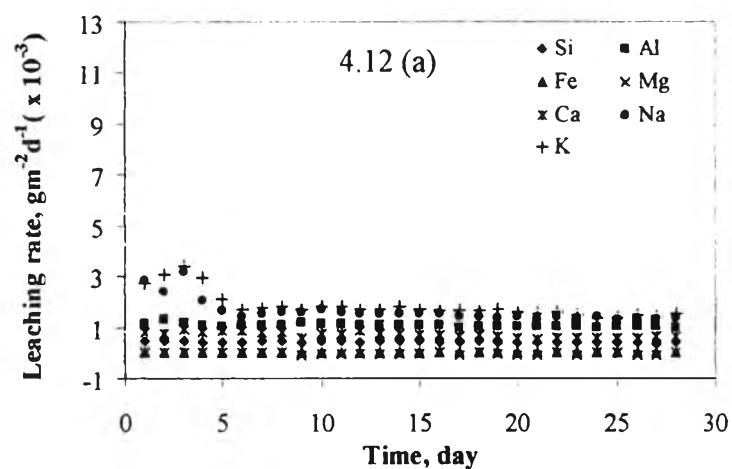
Figure 4.11: Leaching rates of each element as a function of time from the synthetic fly ash F1 at (a) pH = 11.5, (b) pH = 12, and (c) pH = 12.5

Figure 4.11 shows the leaching rate of sample F1 at pH 11.5, 12, and 12.5. The order of the leaching rate was K>Na>Al>Si>Ca>Mg>Fe. At pH 11.5, the leaching rate of each element fluctuated with time. Just as in Class C, the leaching rates of F1 at pH 12 and 12.5 started with low value, increased and reached a maximum value. Then fell off to a lower constant value. The leaching rate increased as the pH of solution increased. The leaching characteristic of F1 followed the same trend as that of C1 but with much lower degree. The leaching rate dropped at early time suggesting the obstruction by precipitate phase occurred very early. It also showed that the silicate or aluminate bonding might be very strong that the hydroxyl ion could not attack and removed the gel for diffusion to proceed at high rate further. This glass was considered the richest Na and K content in the F series.
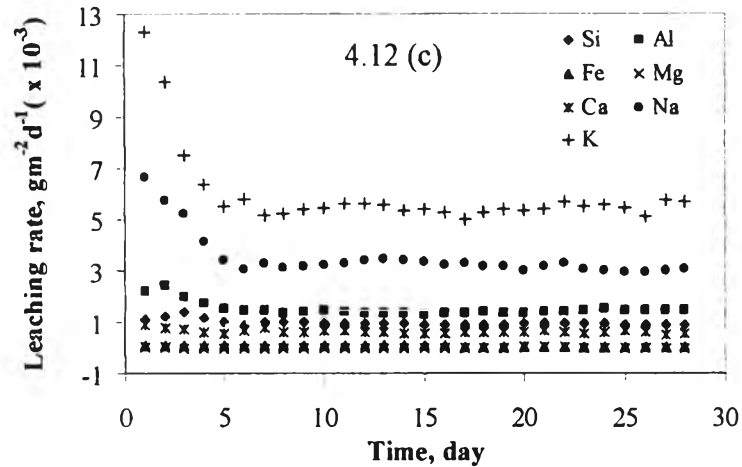
Figure 4.12: Leaching rates of each element as a function of time from the synthetic fly ash F2 at (a) pH = 11.5, (b) pH = 12, and (c) pH = 12.5

Figure 4.12 shows the leaching rate of sample F2 as a function of time at different pH. The order of the leaching rates were K>Na>Al>Ca>Si>Mg>Fe at pH 11.5 and pH 12, but at pH 12.5 the released Si was higher than Ca. As expected, F2 had the same leaching profile as F1 with the lower leaching rate of elements. This was a result of its low Na and K content that rendered the stronger structure.
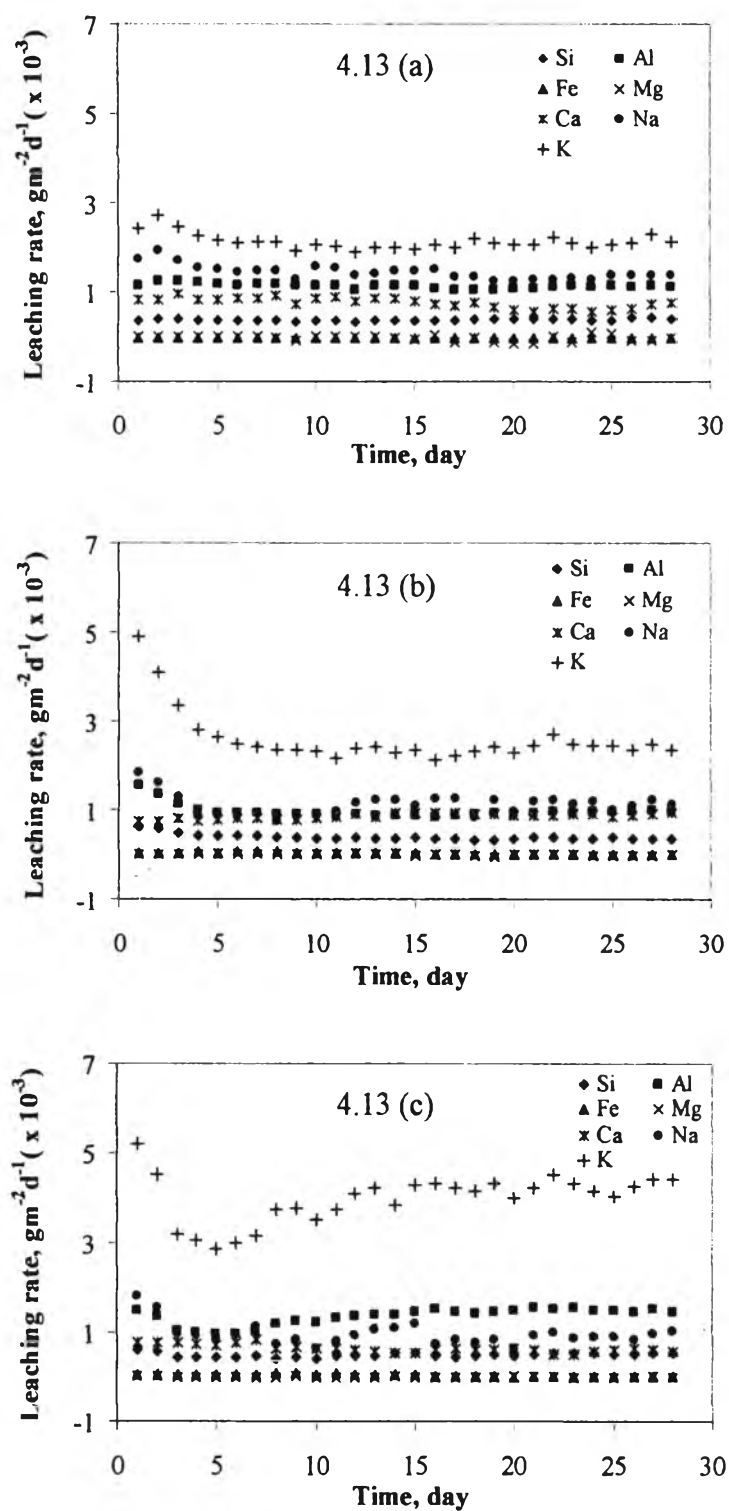
Figure 4.13: Leaching rates of each element as a function of time from the synthetic fly ash F3 at (a) pH = 11.5, (b) pH = 12, and (c) pH = 12.5

The leaching rate of sample F3 at different pH values is shown in Figure 4.13. The order of the leaching rates were K> Na >Al> Ca>Si>Mg>Fe at pH 11.5 and 12, but at pH 12.5 the leaching rate of Al was higher than the leaching rate of Na. The pH had a small effect on leaching rate of this sample. Only the leaching rate of K increased to about 0.001 $gm^{-2}d^{-1}$ when pH increased from 11.5 to 12 and increased to another 0.001 $gm^{-2}d^{-1}$ when the pH increased to 12.5. This might be because the structure of F3 was so strong. Although the pH was very high, the network could not be broken down. By comparing the steady state leaching rate within Class F series found that the order of the leaching rates of Si was F3<F2<F1. Their leaching rate was also in the same order as their alkalis content. Thus, the leaching rate of this series was depended on the alkali contents.

With regard to the effect of Al/Si ratio, the formation of Al-Si as an aluminosilicate structure in glass seems to be more stable than the pure Si structure (Mills, 1993). Moreover the Al^{3+} cation can form a tetrahedral which enhances the overall polymerization of glass. The addition of Al in glass decreases both the ion exchange and matrix dissolution rates. Although silica is a network former and serves as a good measure for determining the dissolution rates of glass, it has been shown that Al/Si ratio serves as a measure to explain the dissolution rate more effectively (Mills, 1993). The glass with higher Al/Si ratios tends to have stronger structures. From the Figure 4.6, Class F had more Al/Si ratio content than Class C, thus, it had higher leaching rate than Class C.

4.3   Effect of pH on leaching rate of synthetic fly ash

The effect of pH on the leaching rate is shown in Figure 4.13 for both Class C and Class F. The leaching rate for silica is used to represent the leaching rate of each sample. This is because silica is the main structure and connection in the glass network. Moreover silica was not found to form as a precipitate in the leachate solution. Thus it is the best measure for the comparison of leaching rate among glasses.
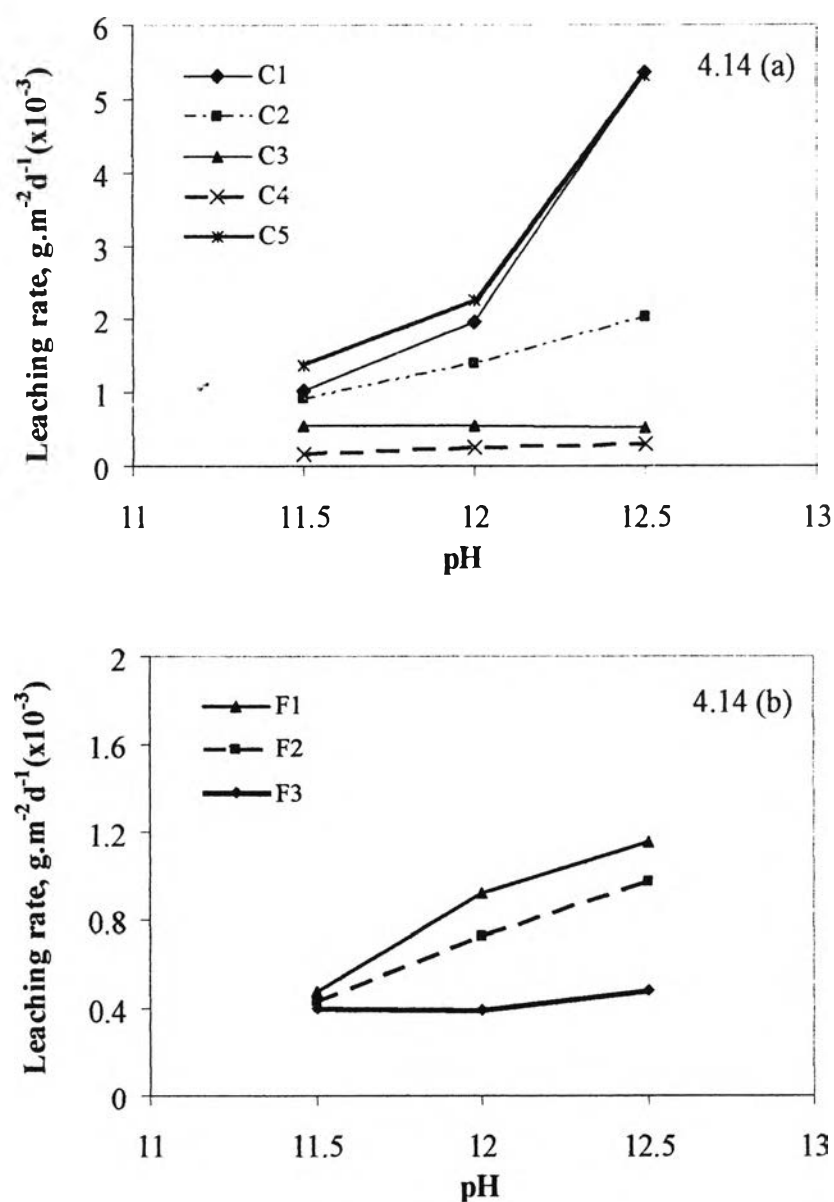

Figure 4.14: Leaching rate of Si at different pH for (a) Class C and (b) Class F.

It is found that the leaching rate of Class C increases with higher pH. On the other hand, the leaching rate of Class F does not vary much with the pH. This might be because the structure of Class F glass is very strong so the high concentration of hydroxide ion at high pH cannot attack its strong structure.

For general glass the single most controlling environmental factor determining whether the predominant mechanism will be ion exchange or etching (congruent) dissolution is the pH of the contact solution. Etching or dissolution dominates in the alkalis regime, increasing dramatically as pH rises (Adams, 1988). The leaching result from this study agrees with this concept. The result shows the important of dissolution at high pH in enhancing the overall leaching rate. It also shows that the diffusion and dissolution occurs simultaneously.

4.4   Kinetic approach of synthetic fly ash

The normalized mass loss of Si as a function of time is plotted in the following figures to determine the kinetic characteristic for the leaching. Moreover the graphs were fitted with diffusion and dissolution equation to find the coefficients of diffusion and dissolution, which are k_1 and k_2 respectively. The data were fit the entire curve with single equation, $F = k_1 t^{1/2} + k_2 t$, because both the diffusion and dissolution mechanisms could proceed simultaneously. The program Origin was used to fit the curve using this defined equation. The coefficient, k_1 and k_2, of the overall sample are shown in the Table 4-5
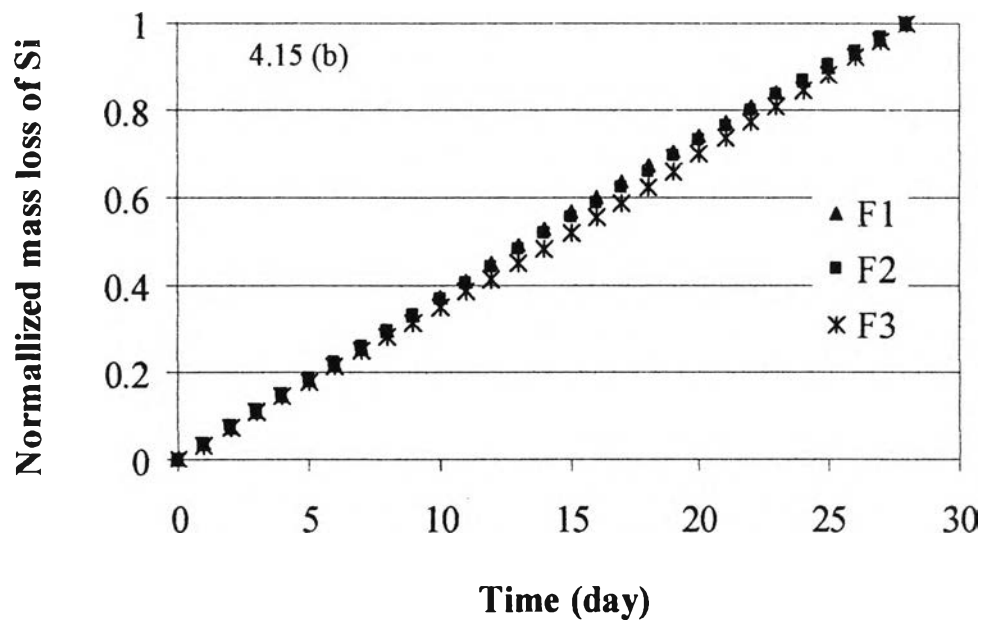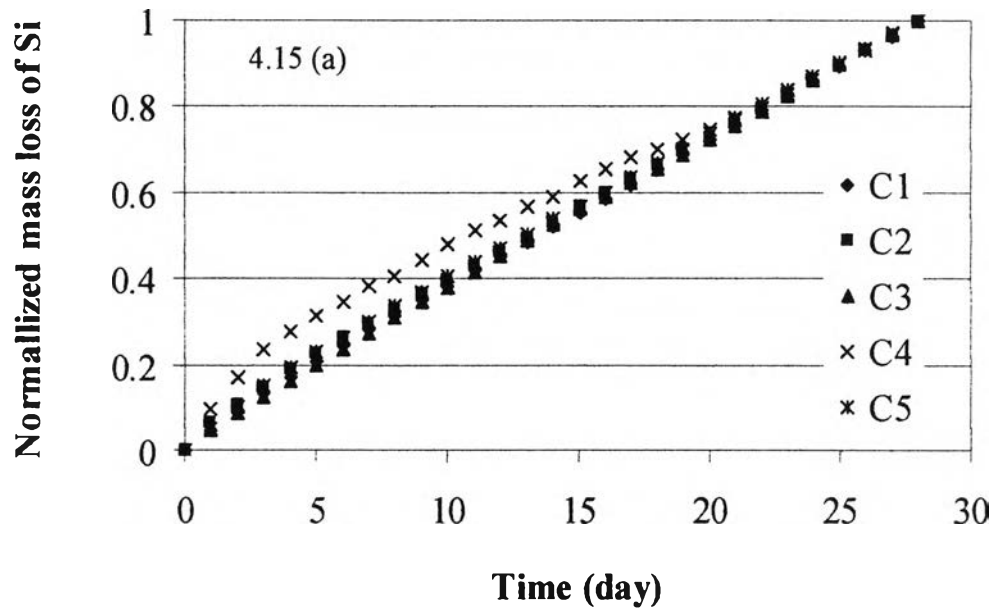
Figure 4.15: Normalized mass loss of silica as a function of time at pH 11.5 for (a) Class C (b) Class F

Figures 4.15 (a) and 4.15 (b) show the normalized mass loss of Si with time at pH 11.5 for Class C and Class F, respectively. They are not zero-order as observed visually. At the beginning, the leaching proceeds at a little faster rate, and then it slightly slows down with time. This is evidence that both diffusion and dissolution take place. The mechanism at the beginning period proceeds with the diffusion mechanism, which is the process where alkalis ions in the glass exchange with the hydronium ions in the solution. After the glass lost some amount of alkalis, the silicate bonding was broken down by a dissolution mechanism. This process was clearly shown at a later period in the normalized mass loss graphs of Class C and Class F at pH 11.5 by the nearly straight line for all samples except C4. The dissolution mechanism was dominant in these glass with the exception of C4.

This conclusion is confirmed by their coefficient value in Table 4-5. For the Class C series, the value of k_1 was slightly different from k_2; but for C4, the value of k_1 was significantly higher than k_2. The C4 had a lower k_2 than the others because its structure was very strong. So its silicate bonding did not breakdown at a high rate. In the Class F series, k_1 for all of them was lower than k_2. This might be because the diffusion reaction occurred on the glass surface only and did not go deep into the bulk glass region.
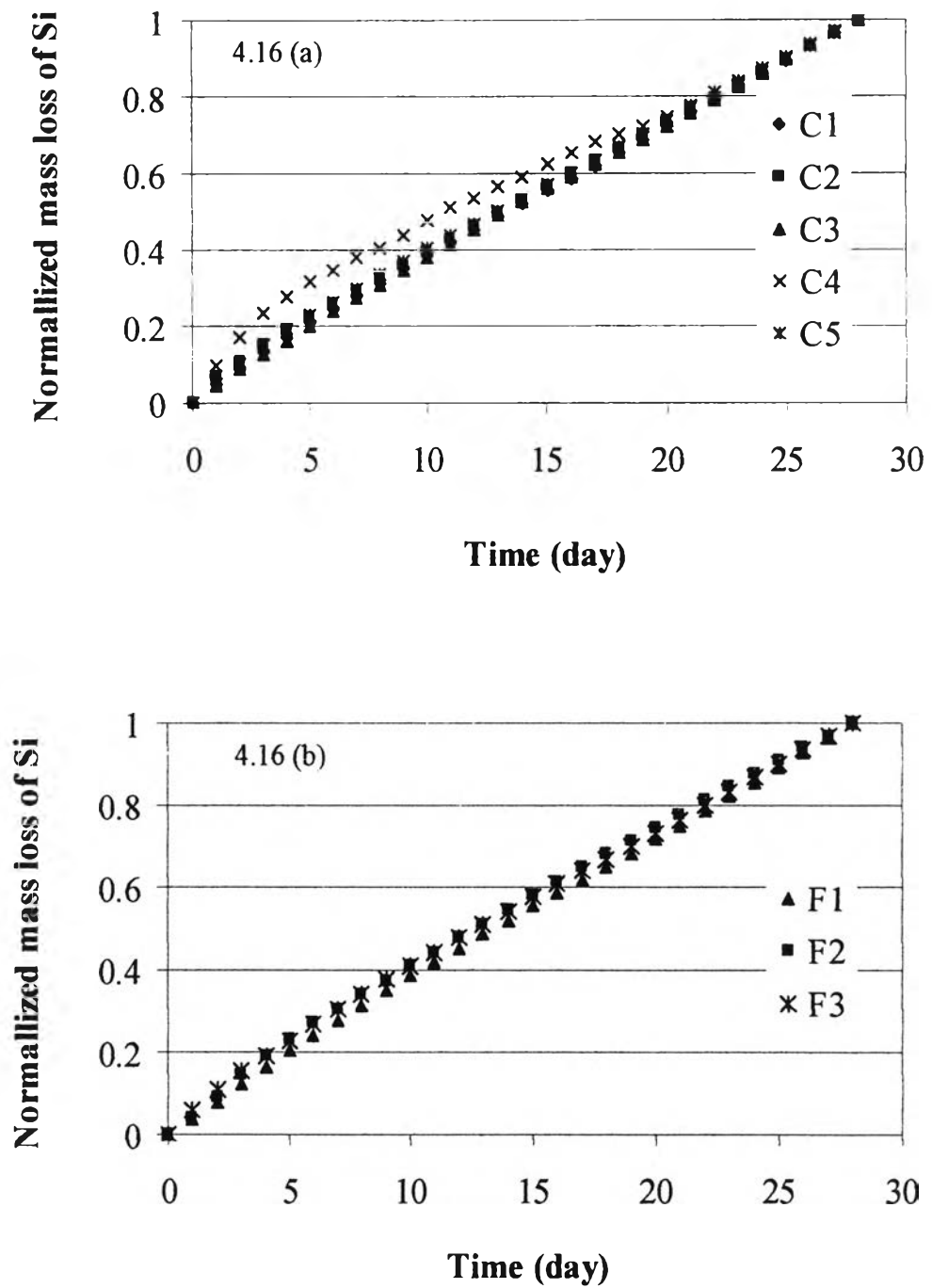
Figure 4.16: Normalized mass loss of silica as a function of time at pH 12 for (a) Class C (b) Class F

Figure 4.16(a) and 4.16(b) show the normalized mass loss of Si with time at pH 12 for Class C and Class F, respectively where a similar trend as in pH 11.5 was observed. Most plots have nearly straight lines, with the exception of C4. The increase in the pH of the solution reduced the diffusion coefficient of C4 but it increased in the Class F samples as presented in Table 4-5. Thus it can be noticed that the plot of Class F is slightly curved at the beginning.
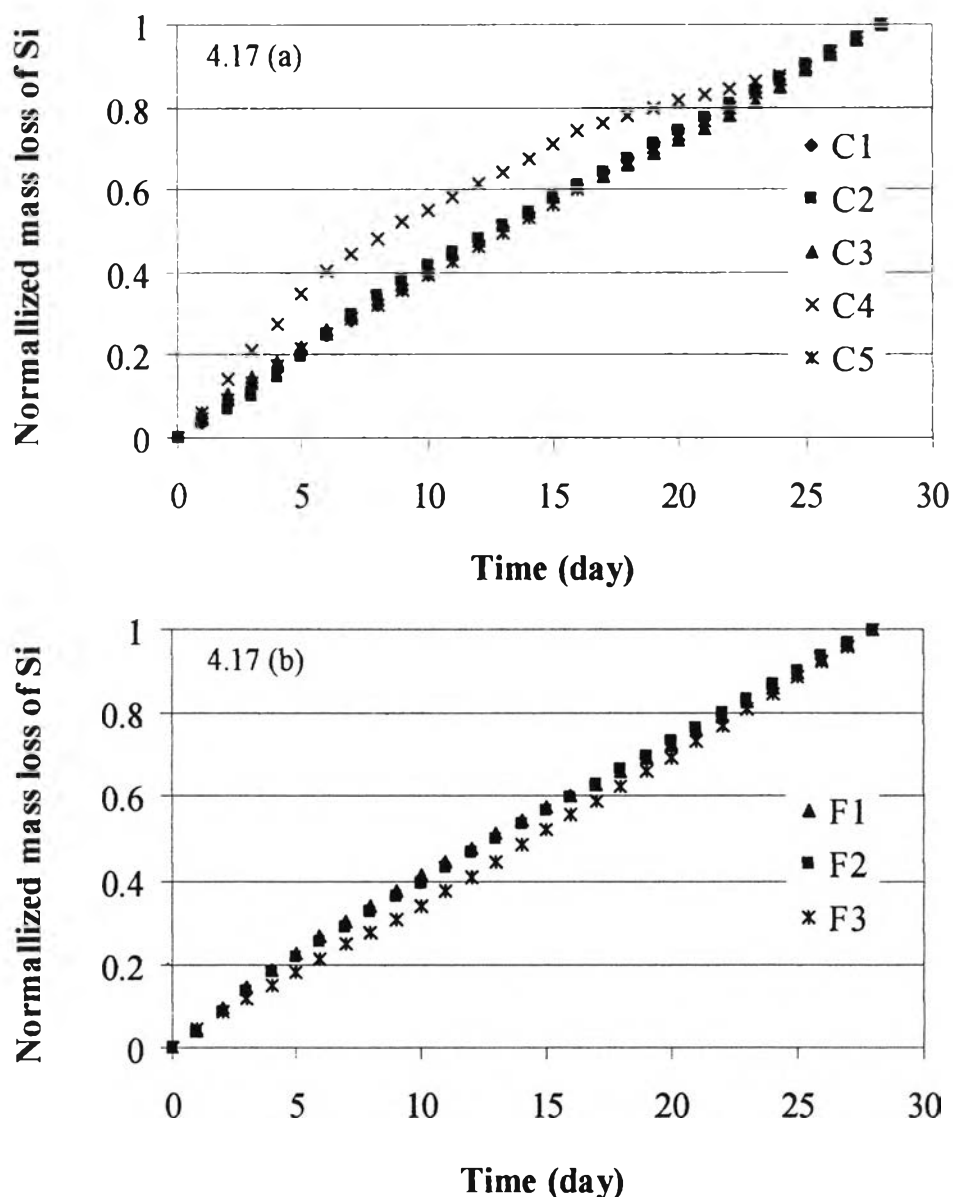

Figure 4.17: Normalized mass loss of silica as a function of time at pH 12.5 for (a) Class C (b) Class F

Figure 4.17(a) and 4.17(b) express the normalized mass loss over time of synthetic fly ash at pH 12.5 for Class C and Class F, respectively. They have the same trend as the lower pH batches but the curvature of line is more noticeable. With regard to the coefficient value in Table 4-5, it is shown that both diffusion and dissolution proceeded at the same rate for all samples, except C4. This might be because C4 has a very strong structure. Although alkalis diffuse out easily, the networks cannot be broken down.

Table 4-5: Diffusion and dissolution coefficient

Sample	pH11.5		pH12		pH12.5	
	k_1	k_2	k_1	k_2	k_1	k_2
F1	0.0080	0.0348	0.0191	0.0319	0.0379	0.0282
F2	0.0076	0.0346	0.0372	0.0289	0.0274	0.0306
F3	0.0000	0.0352	0.0392	0.0281	0.0000	0.0351
C1	0.0213	0.0315	0.0626	0.0241	0.0259	0.0311
C2	0.0343	0.0289	0.0264	0.0308	0.0278	0.0308
C3	0.0177	0.0324	0.0291	0.0294	0.0400	0.0276
C4	0.0999	0.0159	0.0892	0.0189	0.1377	0.0097
C5	0.0359	0.0289	0.0378	0.0287	0.0266	0.0307

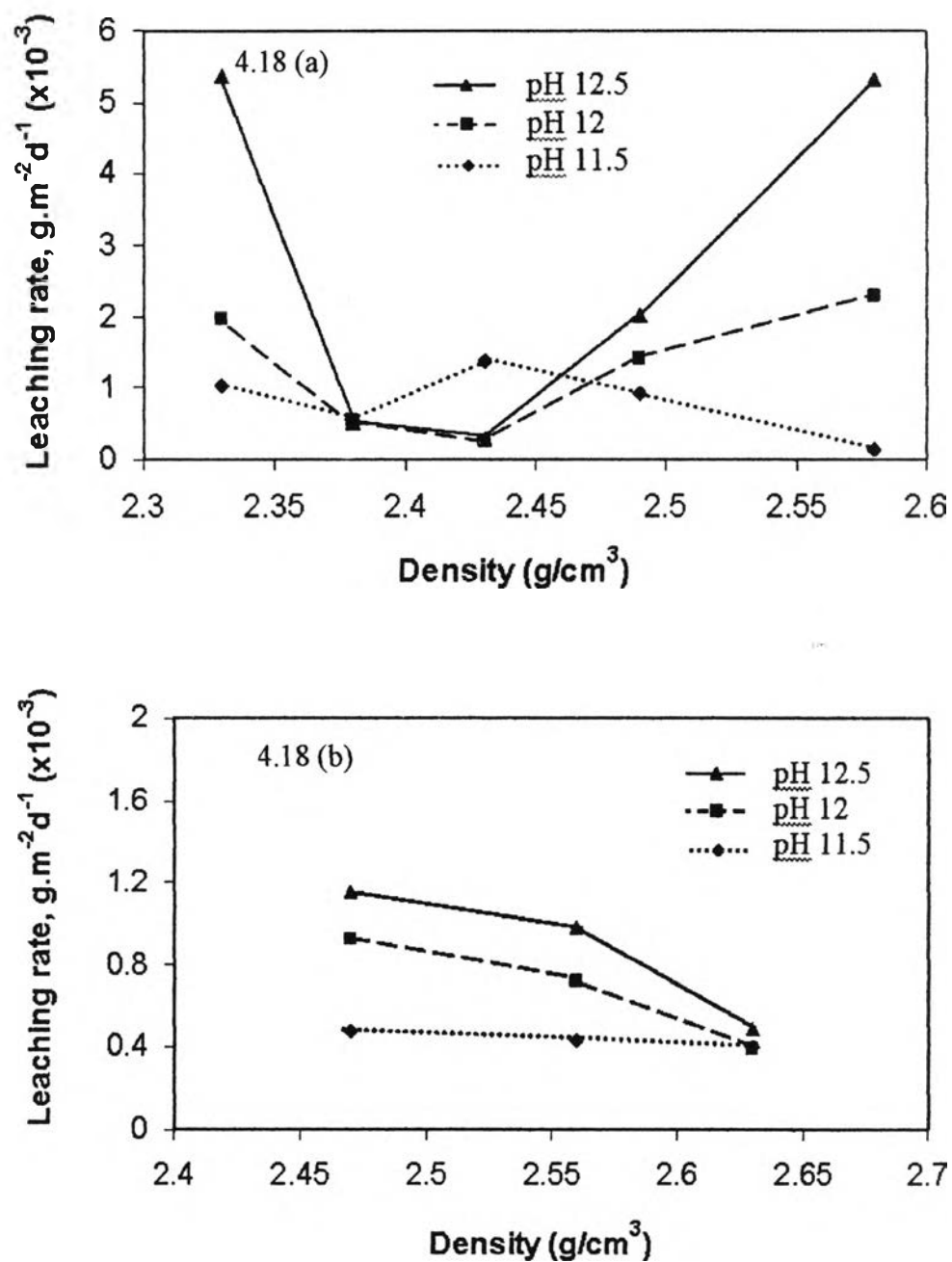**4.5** **The relationship between the density and leaching rate of synthetic fly ash**

Figure 4.18: The relationship between the density and leaching rate of Si of (a) Class C and (b) Class F.

Since density relates to the composition, it might be used as a rough indicator to determine the durability of synthetic fly ash. As shown in Figure 4.18, when the density of the synthetic ash increases, the leaching rate tends to decreases for Class F. This is because the density of glass increases with decreasing alkalis content as shown in Figure 4.4. Glass with lower alkalis content tends to have low the leaching rate. Thus synthetic ash with a high density value should have strong structure and low leaching rate. On the other hand, synthetic fly ash with low density tends to have a lot of openings in its structure and tends to be a good pozzolan. However the density cannot be used as indicator for Class C. It might be because not only density but also other factors varying in Class C might affect the leaching rate.

4.6 Effect of Na$_2$O+K$_2$O on the leaching rate of synthetic fly ash

From the leaching rate section, it can be seen that the alkalis content has a major effect on the mechanism and surface reaction of synthetic fly ash. So it is important to investigate its effect on the dissolution rate thoroughly. The total alkalis content of each sample is shown in Table 4.6 and their correlation on the leaching rate is seen in Figure 4.19.

Table 4-6: Significant oxide ratio

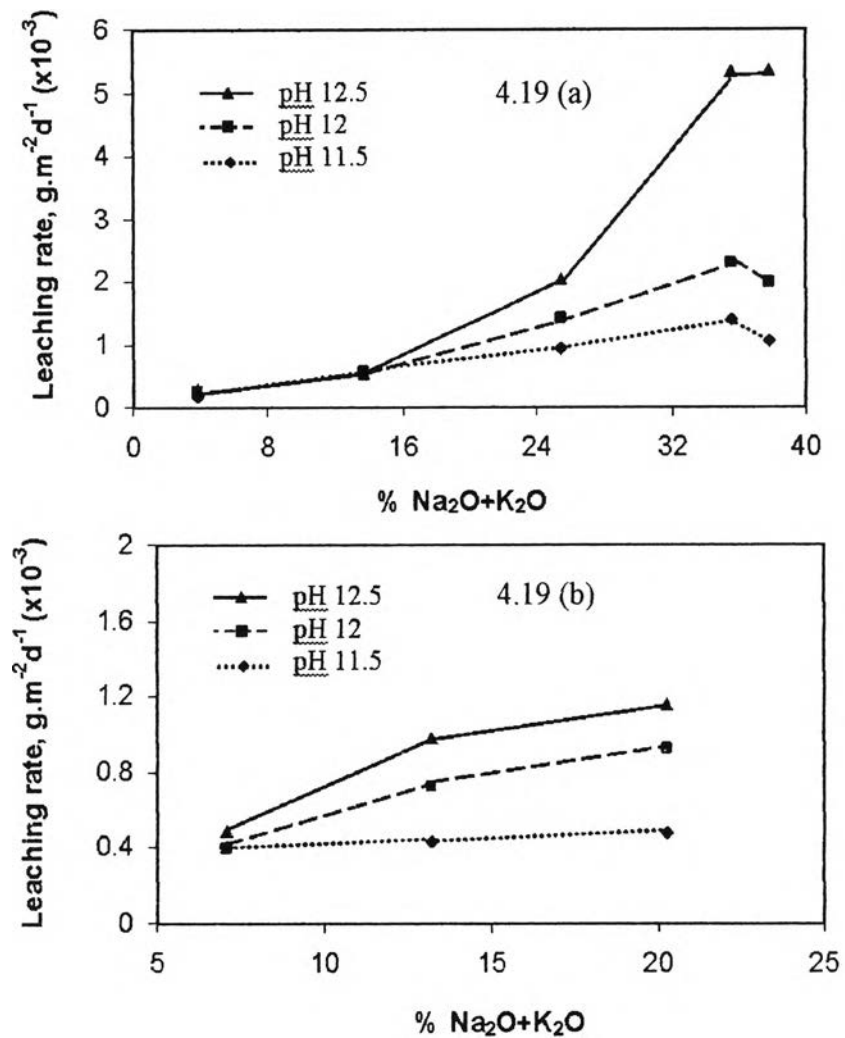| Glass	Na$_2$O+K$_2$O (weight %)	CaO+MgO (weight %)	CaO/Na$_2$O+K$_2$O (weight %)	NBO/T (molar)
C1	37.84	16.22	0.39	1.654
C2	25.47	29.4	1.10	1.87
C3	13.66	41.73	2.94	2.068
C4	3.87	41.21	10.18	1.284
C5	35.53	6.71	0.14	0.796
F1	20.27	9.04	0.37	0.295
F2	13.24	15.51	1.03	0.329
F3	7.1	23.48	3.06	0.452

Figure 4.19: Effect of Na_2O+K_2O on the leaching rate for (a) Class C and (b) Class F.

As expected, the leaching rate of silicate glass increases dramatically with increasing alkalis content. The straight slope in leaching rate of low pH suggests that the diffusion mechanism is dominant and dissolution mechanism hardly proceeds. The steep slope of leaching rate at high pH suggests that dissolution mechanism is taking place at greater rate. It enhances the leaching rate significantly. The steep slope is more obvious in Class C than in Class F fly ash. It can be explained that the Class F has stronger structure that can withstand the OH⁻ attack.

4.7 Effect of alkalis and alkaline earth on leaching rate of Si in synthetic fly ash

To study the effect of alkalis and alkaline earth on the leaching rate, their total percentage is plotted with the leaching rate of Si as shown in Figure 4.20. The total alkalis and alkaline earth content of each sample was shown in Table 4.6
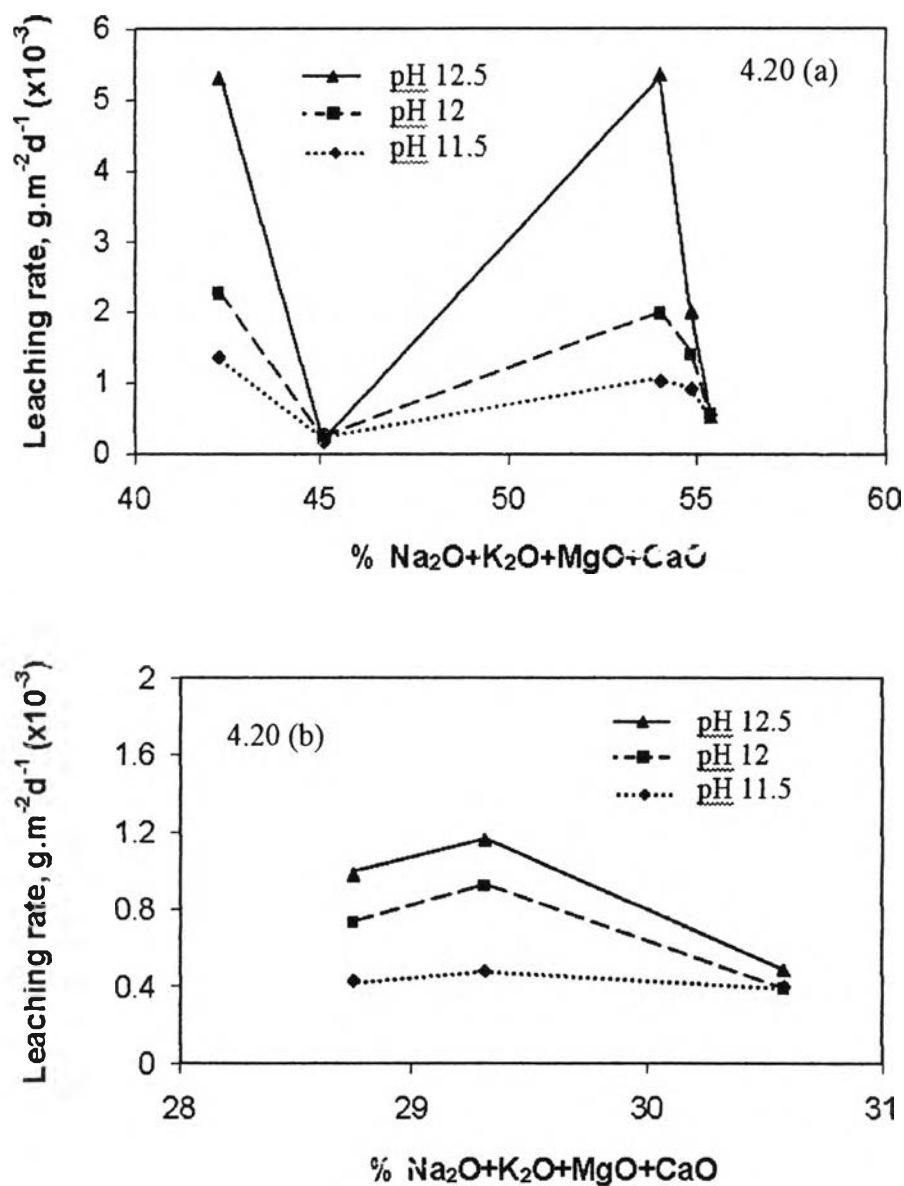

Figure 4.20: Effect of total alkalis and alkaline earth on the leaching rate of Si for (a) Class C and (b) Class F.

As seen in Figure 4.19, there is strong correlation between the alkalis content and the leaching rate. However, when we included alkaline earth content, MgO and CaO, in a parameter, there is no correlation between them as shown in Figure 4.20. This could be because the alkaline earth, Ca and Mg, inhibit the leaching rate of synthetic fly ash. It supports the reason that the presence of Ca can decrease the thickness of the silica-rich layer films, and decrease the dissolution rate of silica. It can also form the secondary film or dual film cover on the surface of glass (Hench, 1988). Another alkaline earth, Mg, is known to reduce silica solubility. It can be highly insoluble on the negatively charged silicate surface (Barkatt, 1988).

4.8 Effect of CaO/Na$_2$O+K$_2$O on leaching rate of synthetic fly ash

The effect of CaO/Na$_2$O+K$_2$O ratio is used to investigate the effect of alkalis and alkaline cations ratio. This is by assuming that Na$_2$O+K$_2$O is a sum of network modifier and CaO is inhibitor. Another reason for this it is in a normalized composition. Thus, a relative ratio should be used to avoid the constant sum constrain where the concentration cannot vary independently. These two types of oxides affect the rate of the reactive components, which are Si and Al, enter into the hydration reaction. The CaO/Na$_2$O+K$_2$O ratio of each sample is shown in Table 4.6 and the effect of the ratio on the leaching rate is shown in the following figures.
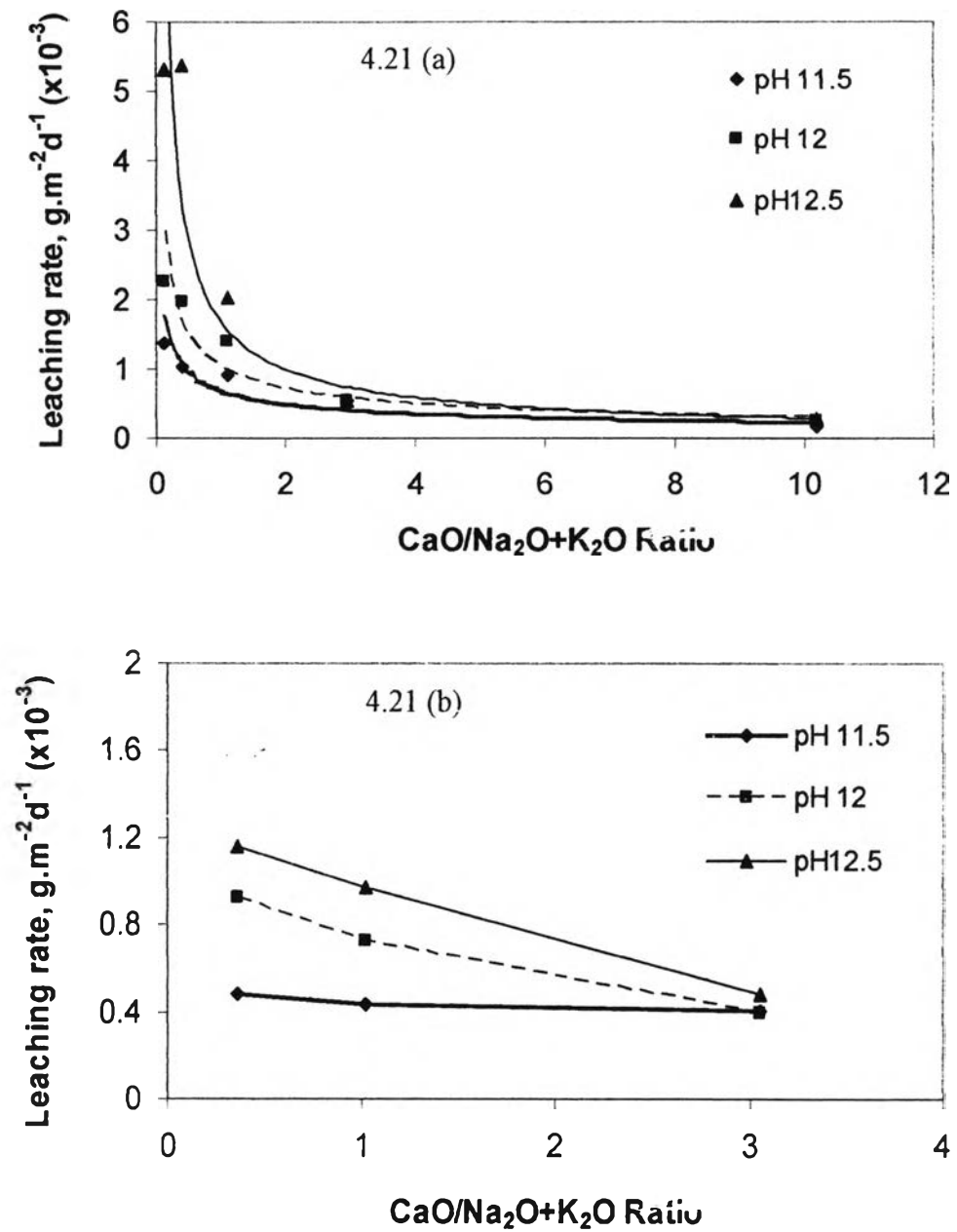
Figure 4.21: The Effect of CaO/Na₂O+K₂O ratio on the leaching rate of Si for (a) Class C and (b) Class F.

From the above Figure, it can be seen that the leaching rate of Si in synthetic fly ash decreases when the CaO/Na_2O+K_2O ratio increase. The drastic reduction is seen up to the ratio of two in Class C. While in Class F, the reduction is less pronounced. The negative effect of the high ratio on the leaching rate can be due to either the effect of the high CaO content or low total alkali and alkaline earth content or both. The glass with high ratio could mean low leaching rate since it has high CaO and low network modifier. As stated earlier, high CaO indicates high possibility of leaching obstruction by calcium phase in subsurface layer. It has been reported that the addition of Ca^{2+} leads to high concentrations of more depolymerised units (Mills, 1993). It can also participate in the formation of a metal silicate compound that forms a protective layer on the glass surface (Adam, 1998). Low network breaker can indicate the strong network structure and less diffusion to form hydrated silicate gel. Therefore, it can be concluded that the CaO/Na_2O+K_2O ratio can be used to estimate the leachability of fly ash.

4.9 Effect of NBO/T ratio on the leaching rate

The NBO/T ratio, the number of non-bridging oxygen per tetrahedrally-coordinated atom, is used to represent the degree of depolymerization of the melt. The NBO/T was calculated by the following formula (Mills, 1993):

$$NBO/T = Y_{NB}/x_T$$

$$Y_{NB} = \Sigma\, 2\, [\, x(CaO)+ x(MgO)+ x(FeO)+ x(MnO)+ x(Na_2O)+ x(K_2O)] +$$
$$[6(1\text{-}f)\, x(Fe_2O_3)] - 2[\, x(Al_2O_3)] - 2f\, [\, x(Fe_2O_3)]$$

$$x_T = \Sigma\, x(SiO_2)+2x(Al_2O_3) + 2fx(Fe_2O_3)+x(TiO_2)+2x(P_2O_5)$$

$$f = Fe^{3+}(IV)/(Fe^{3+}(IV)+Fe^{3+}(VI))$$

Where NBO is non-bridging oxygen, T is the amount of tetrahedrally-coordinated atoms, x is the mole fraction. The NBO/T of each sample is shown in Table 4.6 and the example for NBO/T calculation is shown in Appendix D.
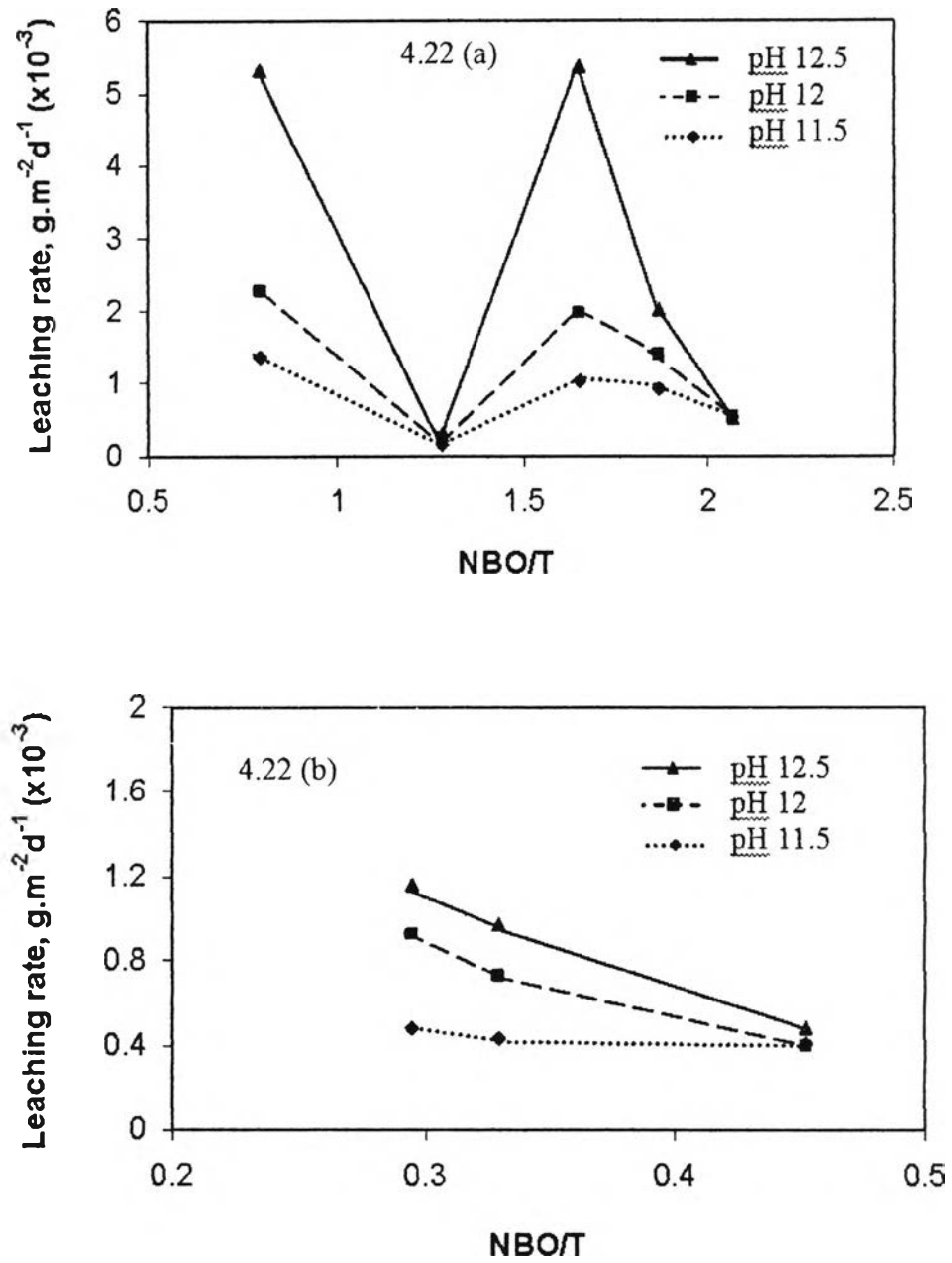
Figure 4.22: The effect of NBO/T on the leaching rate of Si (a) Class C and (b) Class F.

The NBO/T has been used to determine the durability of glass as high NBO content can define discontinuity of glasses. It is associated with both network substitution and the depolymerization of networks by modifier ions (Hemming and Berry, 1988). Also, the increase of NBO leads to an increase in the Na ion-exchange rate (McGrail, 2001). Therefore, glass with a high NBO/T ratio tends to have low connectivity, weak structure, and is easy to dissolve in the solution. However, from Figure 4.22, it can be seen that there is no correlation between NBO/T and leaching rate. This confirms that the leachability of glass is not function of silicate bonding only. But it is also a function of the obstruction by the hydrated silicate gel and Ca and Mg phase.
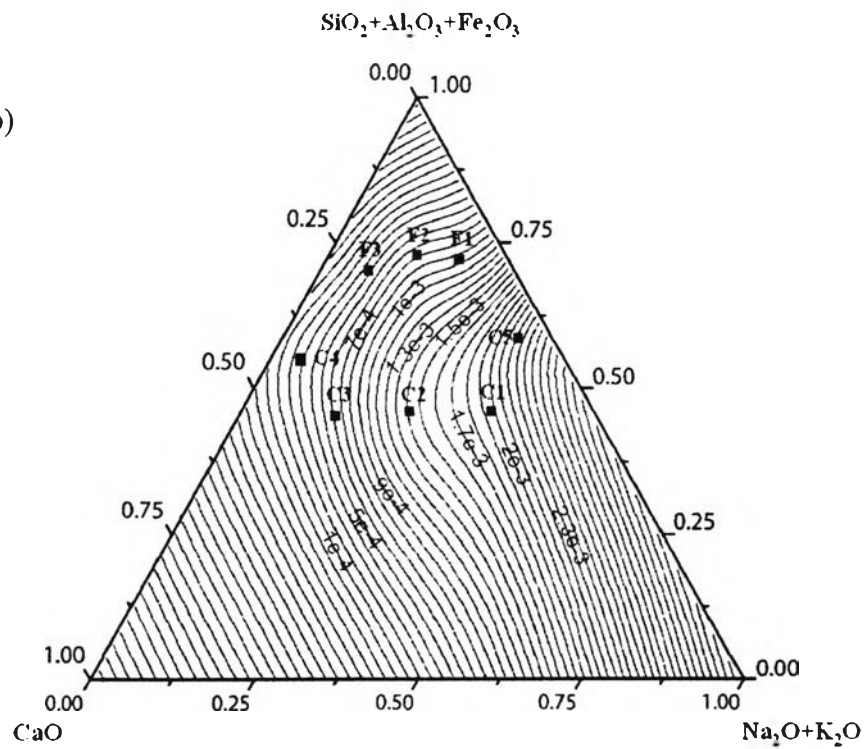
4.10 Ternary Diagram

A ternary diagram is used as a tool to determine the leaching rate of Si from different chemical compositions of synthetic fly ash. It is plotted in glass coordinate with the axes: $SiO_2+Al_2O_3+Fe_2O_3$, Na_2O+K_2O, and CaO, which are known as glass, network formers, network modifiers, and intermediates, respectively. It might be used as primary criteria to assess the reactivity of real fly ash. The leaching rate is shown as the contour line. However the value on the graph is composition of glassy phase. To determine the leaching characteristic of real fly ash, the percentage of glassy phase present in the fly ash is required. Then use the rule of three in arithmetic to calculate the actual leaching rate.
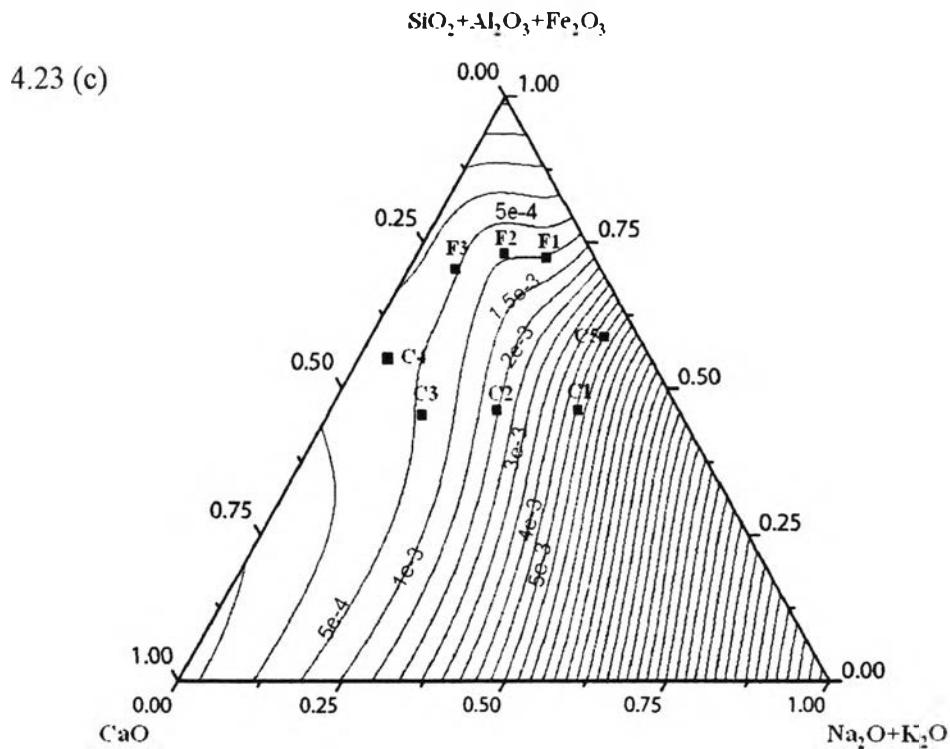
4.23 (a)
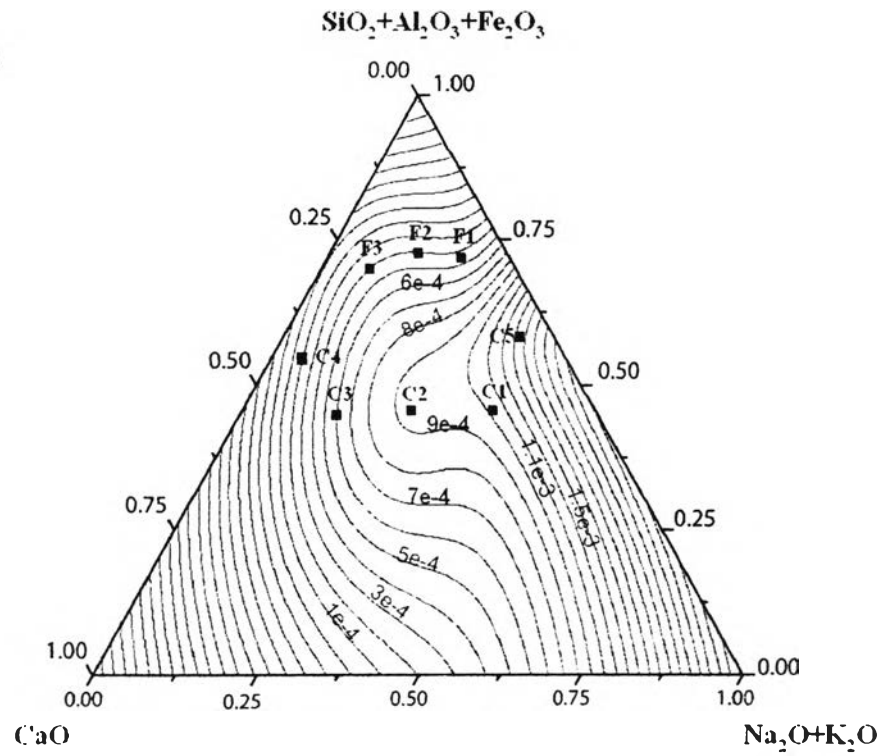
4.23 (b)

Figure 4.23: Ternary diagram of leaching rate (a) pH 11.5, (b) pH12, and (c) pH 12.5

The ternary diagram of leaching rate of different pH is shown in the Figure 4.23. This is a useful method to compare among four parameters, network former, network modifier, and intermediate or inhibitor as we assumed. The leaching rate is used as a measure of reactivity since it is the real amount of silica dissolved to the solution at that pH. However, it needs to be converted to a more common parameter to be used in practice. In this study, it is used to investigate the correlation of relative leaching rate with glass network. It can be seen that at high pH of 12 and 12.5 or at cement pore solution, the leaching rate is high toward high Na and K content. CaO has no effect when it presents in less than 0.12 but has negative effect when it presents in more than 0.12. Network former (SiO_2, Al_2O_3, and Fe_2O_3) has almost no effect when they are less than 0.65, but has negative effect when they are more than 0.65, which is an area of Class F glass.